

**Projector augmented-wave method: Application to relativistic spin-density functional theory**

Andrea Dal Corso

*International School for Advanced Studies (SISSA), Via Bonomea 265, 34136 Trieste, Italy  
and DEMOCRITOS IOM, CNR, Trieste, Italy*

(Received 3 May 2010; revised manuscript received 12 July 2010; published 11 August 2010)

Applying the projector augmented-wave (PAW) method to relativistic spin-density functional theory (RSDFT) we derive PAW Dirac-Kohn-Sham equations for four-component spinor pseudo-wave-functions. The PAW freedom to add a vanishing operator inside the PAW spheres allows us to transform these PAW Dirac-type equations into PAW Pauli-type equations for two-component spinor pseudo-wave-functions. With these wave functions, we get the frozen-core energy as well as the charge and magnetization densities of RSDFT, with errors comparable to the largest between  $1/c^2$  and the transferability error of the PAW data sets. Presently, the latter limits the accuracy of the calculations, not the use of the Pauli-type equations. The theory is validated by applications to isolated atoms of Fe, Pt, and Au, and to the band structure of fcc-Pt, fcc-Au, and ferromagnetic bcc-Fe.

DOI: [10.1103/PhysRevB.82.075116](https://doi.org/10.1103/PhysRevB.82.075116)

PACS number(s): 71.15.Dx, 71.15.Rf, 75.20.En

**I. INTRODUCTION**

After a few years from the proposal of density functional theory (DFT),<sup>1</sup> a relativistic extension able to deal with both nonmagnetic and magnetic systems was presented.<sup>2</sup> Although not free from subtle conceptual issues—a problem that we do not address in this paper—the relativistic theory is at the foundations of most DFT studies of materials. Pseudopotentials (PPs) are constructed starting from the atomic solutions of relativistic DFT (RDFT) equations or of their scalar relativistic (SR) approximation,<sup>3</sup> and all-electron methods deal relativistically with core electrons and often also with valence electrons.<sup>4,5</sup> Formally, the RDFT Kohn-Sham (KS) equations are rather similar to their nonrelativistic counterparts: the kinetic-energy operator is replaced with the Dirac kinetic energy<sup>6</sup> and the wave functions are four-component spinors. Magnetism is treated in the theory assuming that the exchange and correlation energies are functionals of the charge and magnetization densities. The resulting relativistic spin-density functional theory (RSDFT) equations have been solved by many authors in isolated atoms and molecules<sup>7–10</sup> and several codes are available also for solids.<sup>11–13</sup>

Practical calculations of the DFT total energy require a basis set and the plane-wave basis together with the projector augmented-wave (PAW) (Refs. 14–17) method is becoming increasingly popular. The PAW method makes a mapping, exact in principle, between pseudo-wave-functions, described by plane waves, and all-electron wave functions whose rapid oscillations close to the nuclei are treated by introducing spheres about each atom and radial grids inside these spheres. The mapping is carried out with the help of a set of partial waves and projectors calculated in the isolated atoms. This mapping is exact in the limit of a large number of partial waves but in practice a compromise must be made between the partial-wave completeness and the computational efficiency. So far, the PAW method has been used within nonrelativistic DFT,<sup>14–17</sup> although SR effects are included in the PAW data sets and sometimes also spin-orbit effects are calculated.<sup>4,18</sup>

In this paper, we introduce RSDFT within the PAW scheme. We give two formulations of the theory. A fully

relativistic (FR) Dirac-type version and a FR Pauli-type version obtained from the Dirac-type version through approximations that do not worsen the overall accuracy. At the FR level, the theory is quite similar to its nonrelativistic counterpart. Nevertheless, we give here some details of its derivation because, as far as we know, it is absent in the literature. In the relativistic theory, partial waves and projectors are four-component spinors and the PAW RSDFT equations are Dirac-type equations for four-component spinor pseudo-wave-functions with a local effective self-consistent potential and a nonlocal PP. The coefficients of the nonlocal PP are recalculated at each self-consistent iteration with the instantaneous electronic partial occupations, leading to an efficient and accurate picture of the interaction of the valence electrons with the nuclei and core electrons.

After the introduction of the exact relativistic PAW theory, we proceed by showing that often the PAW Dirac-Kohn-Sham equations can be simplified. We show that it would be worthwhile to solve these equations if the transferability errors (TEs) of the PAW data sets and the other numerical errors were kept below  $1/c^2$  (here  $c$  is the speed of light), a task that, although feasible, is quite hard. The TEs of modern PAW data sets are larger than  $1/c^2$  so the PAW Dirac-type equations can be simplified without losing accuracy by keeping the approximation errors below the TEs. The result of these simplifications are PAW Pauli-type equations whose solutions are two-component spinors which are sufficient to evaluate the FR frozen-core energy, as well as the charge and magnetization densities, with an error either of order  $1/c^2$  or comparable to the TE, depending on which is the largest. This is possible because, outside the PAW spheres, the small components of the pseudo-wave-functions are of order  $1/c$  with respect to the large components (independently from the nuclear charge  $Z_l$ ) and we can use Pauli-type equations with an error of order  $1/c^2$  while, inside the PAW spheres, we can remove the small components of the pseudo-wave-functions exploiting the peculiarities of the PAW method and making errors comparable to the TE. As long as the TE is larger than  $1/c^2$ , we can make these approximations without worsening the overall accuracy.

The problem of simplifying the four-component Dirac equations transforming them into two-component Pauli equations has a long history and many approaches have been proposed.<sup>19,20</sup> Usually these methods neglect terms of order  $(v/c)^k$ , where  $v$  is an estimate of the electron velocity. The most common expansion neglects terms with  $k=3$  and includes mass-velocity, Darwin, and spin-orbit terms.<sup>20</sup> Other expansions might retain also higher order terms but when applied to the calculation of the electronic structure these expansions face the problem that close to the nucleus the all-electron potential diverges and the velocity  $v$  becomes of order  $Z_I$ . In heavy atoms  $Z_I/c$  is quite large. In the zero-order regular approximation<sup>21</sup> the problems due to the potential divergence are avoided and the method has been used extensively in molecules and solids.<sup>22,23</sup> In our approach, approximations are used only outside the PAW spheres where  $v \approx 1$  so that, even using Pauli equations with errors of order  $(v/c)^2$ , the final error is of order  $1/c^2$ , does not increase with the nuclear charge  $Z_I$ , and is usually much smaller than  $(Z_I/c)^k$ , even for large  $k$ .

Norm conserving (NC) and ultrasoft (US) (Ref. 24) PPs are well-defined approximations of the PAW method.<sup>15</sup> FR NC-PPs have been known for a long time<sup>25,26</sup> and several applications of the FR US-PPs are already available in the literature as well.<sup>27–32</sup> For NC-PPs, the present work proves the Kleinman's observation that solutions of the Dirac-type equations can be mimicked, with errors of order  $1/c^2$ , by solving Pauli-type equations with a PP tailored on the large components of the solutions of the atomic radial Dirac-type equations.<sup>25,26</sup> In the US case, we obtain the FR US-PPs introduced in Ref. 27 and, in addition, we give a few hints for their construction. Moreover, we explain analytically why FR US-PPs electronic band structures match all-electron RSDFT band structures, a result that we were able to prove only numerically in Ref. 27.

In this paper, we implement the FR PAW Pauli-type formalism and validate it by a few applications. We start with the atomic frozen-core energy and electron energy levels of Fe, Pt, and Au and show transferability tests of the FR PAW data sets. Then the band structures of the face-centered-cubic (fcc) Pt and Au in a few high-symmetry points of the Brillouin zone are compared with the FR all-electron LAPW approach<sup>11</sup> and with the FR US-PPs.<sup>27</sup> Finally, the FR PAW electronic band structures of ferromagnetic body-centered-cubic (bcc) Fe close to the Fermi level are compared with Refs. 33 and 34 where a NC-PP and an all-electron method were employed. We find that the FR PAW method yields total energies and electronic levels that match the all-electron results based on the Dirac-type equations of RSDFT.

This paper is organized as follows. In Sec. I, we summarize the RSDFT and discuss its nonrelativistic limit in an all-electron frozen-core framework and in Sec. II, we summarize the nonrelativistic PAW approach. Section III contains the derivation of the PAW RSDFT equations in their Dirac-type form. In Sec. IV, we discuss how to simplify these equations and transform them into PAW Pauli-type equations for two-component spinor wave functions. Finally, Sec. V contains a few applications of the FR PAW Pauli-type theory. More technical questions are treated in the appendices. Appendix A deals with the generation of the FR PAW

data sets while Appendix B discusses how to perform the summations over the four-component spinor indexes.

## II. RELATIVISTIC SPIN-DENSITY FUNCTIONAL THEORY

The basic variables of relativistic DFT are the charge and the vector current densities, however here we do not use the general theory, but a simplified version (RSDFT) (Refs. 2 and 6) in which the dependence of the total energy on the orbital part of the vector current is neglected and the spin density is the basic variable. Within RSDFT the total energy of a gas of  $N$  interacting electrons in the external potential of fixed nuclei at positions  $\mathbf{R}_I$  can be written as a functional of the four-component spinor one-electron orbitals  $\Psi_{i,\eta}(\mathbf{r})$ ,

$$E_{\text{tot,ae}} = \sum_{i,\eta_1,\eta_2} \langle \Psi_{i,\eta_1} | T_D^{\eta_1,\eta_2} | \Psi_{i,\eta_2} \rangle + E_{\text{xc}}[\rho_e, \mathbf{m}] + E_H[\rho_e + \rho_Z], \quad (1)$$

where  $i$  indicates the occupied states, the index  $\eta$  runs on the four spinor components, and  $T_D^{\eta_1,\eta_2}$  are the components of the Dirac kinetic-energy operator that can be written in terms of the momentum operator  $\mathbf{p} = -i\nabla$  and of the  $4 \times 4$  matrices  $\boldsymbol{\alpha}_k$  ( $k=x,y,z$ ) and  $\boldsymbol{\beta}$ . In Hartree atomic units, and subtracting the electron rest energy, we have<sup>20</sup>

$$T_D = c\boldsymbol{\alpha} \cdot \mathbf{p} + (\boldsymbol{\beta} - \mathbf{1}_{4 \times 4})c^2, \quad (2)$$

where  $\mathbf{1}_{4 \times 4}$  is the  $4 \times 4$  identity matrix and  $c$  is the speed of light, about 137 in atomic unit.<sup>35</sup>  $E_H[\rho_e + \rho_Z]$  is the Hartree energy of the electron ( $\rho_e$ ) and of the nuclear ( $\rho_Z$ ) charge densities whereas  $E_{\text{xc}}[\rho_e, \mathbf{m}]$  are the exchange and correlation energies that depend on the electron  $[\rho_e(\mathbf{r}) = \sum_{i,\eta_1} |\Psi_{i,\eta_1}(\mathbf{r})|^2]$  and on the magnetization densities  $[\mathbf{m}_k(\mathbf{r}) = \mu_B \sum_{i,\eta_1,\eta_2} \Psi_{i,\eta_1}^*(\mathbf{r})(\boldsymbol{\beta}\boldsymbol{\Sigma}_k)^{\eta_1,\eta_2} \Psi_{i,\eta_2}(\mathbf{r})]$ , where  $\boldsymbol{\Sigma}_k/2$  is the spin angular momentum operator and  $\mu_B$  is the Bohr magneton]. Notice that the spin density  $\rho_{\eta_1,\eta_2}(\mathbf{r}) = \sum_i \Psi_{i,\eta_1}^*(\mathbf{r})\Psi_{i,\eta_2}(\mathbf{r})$ , or  $\rho_e(\mathbf{r})$  and  $\mathbf{m}_k(\mathbf{r})$  can be considered as equivalent variables because  $\rho_e(\mathbf{r}) = \sum_{\eta} \rho_{\eta,\eta}(\mathbf{r})$  and  $\mathbf{m}_k(\mathbf{r}) = \mu_B \sum_{\eta_1,\eta_2} \rho_{\eta_1,\eta_2}(\mathbf{r})(\boldsymbol{\beta}\boldsymbol{\Sigma}_k)^{\eta_1,\eta_2}$ .

The valence frozen-core total energy  $E_{\text{tot}}$ , calculated by subtracting from  $E_{\text{tot,ae}}$  the kinetic and the Hartree energies of the core electrons, is given by

$$E_{\text{tot}} = \sum_{i,\eta_1,\eta_2} \langle \Psi_{i,\eta_1} | T_D^{\eta_1,\eta_2} | \Psi_{i,\eta_2} \rangle + E_{\text{xc}}[\rho + \rho_c, \mathbf{m}] + E_H[\rho] + \int d^3r V_{\text{loc}}(\mathbf{r})\rho(\mathbf{r}) + U_{I,I}, \quad (3)$$

where now the index  $i$  runs on the valence states only,  $\rho$  and  $\rho_c$  indicate the valence and core charge densities,  $V_{\text{loc}} = V_H[\rho_Z + \rho_c]$  is the Coulomb potential of the core and nuclear charges, and  $U_{I,I}$  is the long-range ion-ion interaction energy.

The minimization of this functional leads to the Dirac-type relativistic KS equations,<sup>6</sup>

$$\sum_{\eta_2} \{ T_D^{\eta_1,\eta_2} + [V_{\text{eff}}(\mathbf{r}) - \varepsilon_i] \delta^{\eta_1,\eta_2} - \mu_B \mathbf{B}_{\text{xc}}(\mathbf{r}) \cdot (\boldsymbol{\beta}\boldsymbol{\Sigma})^{\eta_1,\eta_2} \} | \Psi_{i,\eta_2} \rangle = 0, \quad (4)$$

where the effective potential  $V_{\text{eff}}(\mathbf{r}) = V_{\text{loc}}(\mathbf{r}) + V_H(\mathbf{r}) + V_{\text{xc}}(\mathbf{r})$

is the sum of the local, Hartree and exchange and correlation potentials, and  $\mathbf{B}_{xc}(\mathbf{r}) = -\delta E_{xc}/\delta \mathbf{m}$  is the exchange and correlation magnetic fields.  $V_H(\mathbf{r})$  is the Hartree potential of the valence electrons only whereas  $V_{xc}(\mathbf{r})$  and  $\mathbf{B}_{xc}(\mathbf{r})$  are calculated with the total electron charge and magnetization densities. For latter convenience, we define  $V_{\text{LOC}}^{\eta_1, \eta_2}(\mathbf{r}) = V_{\text{eff}}(\mathbf{r})\delta^{\eta_1, \eta_2} - \mu_B \mathbf{B}_{xc}(\mathbf{r}) \cdot (\boldsymbol{\beta} \boldsymbol{\Sigma})^{\eta_1, \eta_2}$ .

The Dirac-type KS equations [Eq. (4)] can be rewritten introducing the large and the small components of the all-electron wave functions,

$$|\Psi_{i,\gamma}\rangle = \begin{pmatrix} |\Psi_{i,\sigma}^A\rangle \\ |\Psi_{i,\sigma}^B\rangle \end{pmatrix}, \quad (5)$$

where  $|\Psi_{i,\sigma}^A\rangle$  and  $|\Psi_{i,\sigma}^B\rangle$  are two-component spinors and the index  $\sigma$  runs on the two components. With the help of the Pauli matrices ( $\boldsymbol{\sigma}$ ) representation of the  $\boldsymbol{\alpha}$  and  $\boldsymbol{\beta}$  matrices, Eq. (4) becomes

$$\sum_{\sigma_2} \{c \boldsymbol{\sigma}^{\sigma_1, \sigma_2} \cdot \mathbf{p} \Psi_{i,\sigma_2}^B(\mathbf{r}) + [V_{\text{LOC}}^{\sigma_1, \sigma_2}(\mathbf{r}) - \varepsilon_i \delta^{\sigma_1, \sigma_2}] \Psi_{i,\sigma_2}^A(\mathbf{r})\} = 0, \quad (6)$$

$$\sum_{\sigma_2} \{c \boldsymbol{\sigma}^{\sigma_1, \sigma_2} \cdot \mathbf{p} \Psi_{i,\sigma_2}^A(\mathbf{r}) + [\bar{V}_{\text{LOC}}^{\sigma_1, \sigma_2}(\mathbf{r}) - (\varepsilon_i + 2c^2) \delta^{\sigma_1, \sigma_2}] \Psi_{i,\sigma_2}^B(\mathbf{r})\} = 0, \quad (7)$$

where now  $V_{\text{LOC}}^{\sigma_1, \sigma_2}(\mathbf{r}) = V_{\text{eff}}(\mathbf{r})\delta^{\sigma_1, \sigma_2} - \mu_B \mathbf{B}_{xc}(\mathbf{r}) \cdot \boldsymbol{\sigma}^{\sigma_1, \sigma_2}$  and  $\bar{V}_{\text{LOC}}^{\sigma_1, \sigma_2}(\mathbf{r}) = V_{\text{eff}}(\mathbf{r})\delta^{\sigma_1, \sigma_2} + \mu_B \mathbf{B}_{xc}(\mathbf{r}) \cdot \boldsymbol{\sigma}^{\sigma_1, \sigma_2}$ .

### Nonrelativistic limit: The Pauli equations

When the electron speed is much smaller than  $c$ , these equations can be approximated by the Pauli equations. From Eq. (7) we get

$$\Psi_{i,\sigma_1}^B(\mathbf{r}) = - \sum_{\sigma_2} [\bar{V}_{\text{LOC}}(\mathbf{r}) - (\varepsilon_i + 2c^2) \mathbf{1}_{2 \times 2}]_{\sigma_1, \sigma_2}^{-1} \times \sum_{\sigma_3} c \boldsymbol{\sigma}^{\sigma_2, \sigma_3} \cdot \mathbf{p} \Psi_{i,\sigma_3}^A(\mathbf{r}). \quad (8)$$

The diagonal elements of the matrix  $\varepsilon_i \mathbf{1}_{2 \times 2} - \bar{V}_{\text{LOC}}(\mathbf{r})$  are comparable to the electron kinetic energy and the off-diagonal elements are of the same order or smaller. In the regions where these elements are small with respect to  $2c^2$ , we can approximate

$$\Psi_{i,\sigma_1}^B(\mathbf{r}) \approx \sum_{\sigma_2} \frac{\boldsymbol{\sigma}^{\sigma_1, \sigma_2} \cdot \mathbf{p}}{2c} \Psi_{i,\sigma_2}^A(\mathbf{r}) \quad (9)$$

with a position-dependent error of order  $[v(\mathbf{r})/c]^3$ , where  $v$  is a parameter of magnitude comparable with the speed of the electron in that region. By inserting Eq. (9) in Eq. (6) we get the Pauli equations,

$$\sum_{\sigma_2} \left[ \frac{\mathbf{p}^2}{2} \delta^{\sigma_1, \sigma_2} + V_{\text{LOC}}^{\sigma_1, \sigma_2}(\mathbf{r}) - \varepsilon_i \delta^{\sigma_1, \sigma_2} \right] \Psi_{i,\sigma_2}^A(\mathbf{r}) = 0, \quad (10)$$

that have an error of order  $(v/c)^2$ . Notice that the solutions of the Dirac equations  $\Psi_{i,\gamma}(\mathbf{r})$  are normalized. This means that

$\sum_{\sigma} \int_V d^3r (|\Psi_{i,\sigma}^A(\mathbf{r})|^2 + |\Psi_{i,\sigma}^B(\mathbf{r})|^2) = 1$ . Therefore  $\Psi_{i,\sigma}^A(\mathbf{r})$  is not normalized. However the missing term is of order  $(v/c)^2$ , the same order of the error of the Pauli equations and can be consistently neglected. For an electron close to an heavy nucleus of charge  $Z_I$ , a good estimate is  $v \approx Z_I$  and  $(Z_I/c)^2$  might be sizable. For the valence states, the nuclear potential is screened so  $v$  is significantly lower than  $Z_I$ . Nevertheless, the use of Eq. (10) in the regions close to the nuclei leads to significant errors. Actually the mass-velocity, Darwin, and spin-orbit terms are neglected in Eq. (10) so spin-orbit splittings are completely missing. On the contrary, in the regions far from the nuclei or for light elements, Eq. (10) is a quite good approximation of Eqs. (6) and (7). The Pauli-type KS equations can be obtained directly from the minimization of the nonrelativistic DFT total energy written for two-component spinor wave functions and used to deal with noncollinear magnetic structures<sup>36</sup>

$$E_{\text{tot, nr}} = \sum_{i,\sigma_1} \langle \Psi_{i,\sigma_1}^A | \frac{\mathbf{p}^2}{2} | \Psi_{i,\sigma_1}^A \rangle + E_{xc}[\rho + \rho_c, \mathbf{m}] + E_H[\rho] + \int d^3r V_{\text{loc}}(\mathbf{r}) \rho(\mathbf{r}) + U_{I,J}, \quad (11)$$

where the charge density is  $\rho(\mathbf{r}) = \sum_{i,\sigma} |\Psi_{i,\sigma}^A(\mathbf{r})|^2$  and the magnetization density is  $\mathbf{m}_k(\mathbf{r}) = \mu_B \sum_{i,\sigma_1, \sigma_2} \Psi_{i,\sigma_1}^{A,*}(\mathbf{r}) (\boldsymbol{\sigma}_k)^{\sigma_1, \sigma_2} \Psi_{i,\sigma_2}^A(\mathbf{r})$ .

### III. NONRELATIVISTIC PAW METHOD

In the nonrelativistic PAW approach<sup>14–16</sup> to the electronic structure problem, the PAW method is used to calculate the energy in Eq. (11). We summarize in this section the main features of the nonrelativistic PAW method following the general scheme presented in Ref. 16 to deal with noncollinear magnetic structures. The approaches to noncollinear magnetism implemented in Ref. 37 using US-PPs, or in Ref. 38 using NC-PPs, are approximations of this PAW formulation. In the PAW approach, a linear mapping transforms the pseudo-wave-functions  $|\tilde{\Psi}_{i,\sigma}^A\rangle$ , which are the variational variables, into all-electron wave functions  $|\Psi_{i,\sigma}^A\rangle$ ,

$$|\Psi_{i,\sigma}^A\rangle = |\tilde{\Psi}_{i,\sigma}^A\rangle + \sum_{l,m} [|\Phi_m^{l,AE}\rangle - |\Phi_m^{l,PS}\rangle] \langle \beta_m^l | \tilde{\Psi}_{i,\sigma}^A \rangle. \quad (12)$$

The mapping requires three sets of functions: the all-electron partial waves  $|\Phi_m^{l,AE}\rangle$ , the pseudo-partial-waves  $|\Phi_m^{l,PS}\rangle$  and the projector functions  $|\beta_m^l\rangle$ . The all-electron partial waves are calculated in an isolated nonmagnetic atom by solving the nonrelativistic Kohn and Sham equations in spherical geometry at  $N_\epsilon$  values of the energy, for a number of orbital angular momenta  $l$ . Therefore the index  $l$  in  $|\Phi_m^{l,AE}\rangle$  indicates the atom and means that the function is centered about the atom at  $\mathbf{R}_l$  and  $m$  is a composite index that indicates  $\tau, l, m_l$ , where  $1 < \tau < N_\epsilon$  identifies the energy,  $0 < l < l_{\text{max}}$  indicates the orbital angular momentum and  $-l < m_l < l$  indicates the projection of the orbital angular momentum on a quantization axis. Each pseudo-partial-wave coincides with the corresponding all-electron partial wave outside a given cutoff radius and is smoothly continued by a pseudization recipe

inside the cutoff radius. For each atom, the maximum cutoff radius defines the size of the PAW sphere. The projector functions are orthogonal to the pseudo-partial-waves  $\langle \beta_n^I | \Phi_m^{I,PS} \rangle = \delta_{nm}$  and are localized inside the PAW sphere. The accuracy of this mapping can be increased systematically by increasing  $N_\epsilon$  and  $l_{\max}$  and when these are sufficiently large the mapping is virtually exact, meaning that inside the PAW sphere

$$\sum_m |\Phi_m^{I,PS} \rangle \langle \beta_m^I| = 1 \quad (13)$$

when applied to any pseudo-wave-function.

Using the above mapping, and the completeness relationship [Eq. (13)], one can prove that the expectation value of a local operator  $A$  that acts on all-electron wave functions can be calculated as the expectation value of a new operator  $\tilde{A}$  that acts on pseudo-wave-functions and is given by<sup>14</sup>

$$\tilde{A} = A + \sum_{l,mn} |\beta_m^I \rangle \langle \Phi_m^{I,AE} | A | \Phi_n^{I,AE} \rangle - \langle \Phi_m^{I,PS} | A | \Phi_n^{I,PS} \rangle \langle \beta_n^I|. \quad (14)$$

The operator  $\tilde{A}$  is not completely determined by the method. There is still the additional freedom to add a term of the form

$$\Delta = B - \sum_{l,mn} |\beta_m^I \rangle \langle \Phi_m^{I,PS} | B | \Phi_n^{I,PS} \rangle \langle \beta_n^I|, \quad (15)$$

where  $B$  is an arbitrary operator localized inside the PAW spheres. This is due to the fact that, using Eq. (13), inside the PAW spheres, we have  $\sum_n |\Phi_n^{I,PS} \rangle \langle \beta_n^I | \tilde{\Psi}_{i,\sigma}^A \rangle = |\tilde{\Psi}_{i,\sigma}^A \rangle$  and therefore  $\sum_\sigma \langle \tilde{\Psi}_{i,\sigma}^A | \Delta | \tilde{\Psi}_{j,\sigma}^A \rangle = 0$ .

Using Eq. (14) with the operator  $A = |\mathbf{r}\rangle \langle \mathbf{r}|$ , one obtains the PAW expression of the spin-density matrix that is composed by three terms:  $\rho_{\sigma_1, \sigma_2}(\mathbf{r}) = \tilde{\rho}_{\sigma_1, \sigma_2}(\mathbf{r}) + \sum_I \rho_{\sigma_1, \sigma_2}^{1,I}(\mathbf{r}) - \sum_I \tilde{\rho}_{\sigma_1, \sigma_2}^{1,I}(\mathbf{r})$ , where the first term is calculated in real space while the other two terms are calculated inside the PAW spheres on radial grids. We have<sup>16</sup>

$$\tilde{\rho}_{\sigma_1, \sigma_2}(\mathbf{r}) = \sum_i \langle \tilde{\Psi}_{i, \sigma_1}^A | \mathbf{r} \rangle \langle \mathbf{r} | \tilde{\Psi}_{i, \sigma_2}^A \rangle, \quad (16)$$

$$\rho_{\sigma_1, \sigma_2}^{1,I}(\mathbf{r}) = \sum_{mn} \rho_{mn}^{I, \sigma_1, \sigma_2} \langle \Phi_m^{I,AE} | \mathbf{r} \rangle \langle \mathbf{r} | \Phi_n^{I,AE} \rangle, \quad (17)$$

$$\tilde{\rho}_{\sigma_1, \sigma_2}^{1,I}(\mathbf{r}) = \sum_{mn} \rho_{mn}^{I, \sigma_1, \sigma_2} \langle \Phi_m^{I,PS} | \mathbf{r} \rangle \langle \mathbf{r} | \Phi_n^{I,PS} \rangle, \quad (18)$$

where the partial occupations are defined as

$$\rho_{mn}^{I, \sigma_1, \sigma_2} = \sum_i \langle \tilde{\Psi}_{i, \sigma_1}^A | \beta_m^I \rangle \langle \beta_n^I | \tilde{\Psi}_{i, \sigma_2}^A \rangle. \quad (19)$$

From the spin-density matrix, the charge and magnetization densities are obtained readily as  $\rho(\mathbf{r}) = \sum_\sigma \rho_{\sigma, \sigma}(\mathbf{r})$  and  $\mathbf{m}_k(\mathbf{r}) = \mu_B \sum_{\sigma_1, \sigma_2} \rho_{\sigma_1, \sigma_2}(\mathbf{r}) (\boldsymbol{\sigma}_k)^{\sigma_1, \sigma_2}$ . With obvious generalizations we can define also  $\tilde{\rho}(\mathbf{r})$  and  $\tilde{\mathbf{m}}_k(\mathbf{r})$  on the real-space mesh, and  $\rho^{1,I}(\mathbf{r})$ ,  $\mathbf{m}_k^{1,I}(\mathbf{r})$ ,  $\tilde{\rho}^{1,I}(\mathbf{r})$ , and  $\tilde{\mathbf{m}}_k^{1,I}(\mathbf{r})$  inside the spheres.

As written, the charge calculated in the real-space mesh integrating  $\tilde{\rho}(\mathbf{r})$  on all space is not equal to the number of

electrons. Its actual value depends on the pseudization procedure of the pseudo-partial-waves. In order to simplify the calculation of the electrostatic energy, it is convenient to introduce compensation charges equal to  $\hat{\rho}^I(\mathbf{r}) = \sum_{mn} \rho_{mn}^I \hat{Q}_{mn}^I(\mathbf{r})$  inside the PAW spheres ( $\rho_{mn}^I = \sum_\sigma \rho_{mn}^{I, \sigma, \sigma}$ ) and to  $\hat{\rho}(\mathbf{r}) = \sum_I \hat{\rho}^I(\mathbf{r} - \mathbf{R}_I)$  in the real-space mesh, such that inside each sphere  $\hat{\rho}^I(\mathbf{r})$  has not only the same charge but also the same multipole moments as  $\rho^{1,I}(\mathbf{r}) - \tilde{\rho}^{1,I}(\mathbf{r})$ . The augmentation functions  $\hat{Q}_{mn}^I(\mathbf{r})$  are determined in such a way to satisfy this constraint as explained for instance in Ref. 15. Using the same augmentation functions we can define the compensation spin density:  $\hat{\rho}_{\sigma_1, \sigma_2}^{1,I}(\mathbf{r}) = \sum_{mn} \rho_{mn}^{I, \sigma_1, \sigma_2} \hat{Q}_{mn}^I(\mathbf{r})$ , and hence the compensation magnetization density  $\hat{\mathbf{m}}_k^{1,I}(\mathbf{r})$  inside the spheres and  $\hat{\mathbf{m}}_k(\mathbf{r}) = \sum_I \hat{\mathbf{m}}_k^{1,I}(\mathbf{r} - \mathbf{R}_I)$  in the real-space mesh.

Using the relationship between all-electron and pseudo-wave-functions, the definition of the operators in Eq. (14), and the decomposition of the electrostatic energy discussed in Ref. 15, the frozen-core energy [Eq. (11)] can be written in terms of pseudo-wave-functions as a sum of three terms, the first calculated in real space and the other two calculated on the radial grids inside the spheres:  $E_{\text{tot}} = \tilde{E} + E^1 - \tilde{E}^1$  with<sup>16</sup>

$$\begin{aligned} \tilde{E} = & \sum_{i,\sigma} \langle \tilde{\Psi}_{i,\sigma}^A | \frac{\mathbf{p}^2}{2} | \tilde{\Psi}_{i,\sigma}^A \rangle + E_{\text{xc}}[\tilde{\rho} + \hat{\rho} + \tilde{\rho}_c, \tilde{\mathbf{m}} + \hat{\mathbf{m}}] + E_H[\tilde{\rho} + \hat{\rho}] \\ & + \int d^3r \tilde{V}_{\text{loc}}(\mathbf{r}) [\tilde{\rho}(\mathbf{r}) + \hat{\rho}(\mathbf{r})] + U_{I,I}, \end{aligned} \quad (20)$$

$$\begin{aligned} \tilde{E}^1 = & \sum_{l,mn} \rho_{mn}^l \langle \Phi_m^{I,PS} | \frac{\mathbf{p}^2}{2} | \Phi_n^{I,PS} \rangle \\ & + \sum_I E_{\text{xc}}[\tilde{\rho}^{1,I} + \hat{\rho}^I + \tilde{\rho}_c^I, \tilde{\mathbf{m}}^{1,I} + \hat{\mathbf{m}}^{1,I}] + \sum_I E_H[\tilde{\rho}^{1,I} + \hat{\rho}^I] \\ & + \sum_I \int_{\Omega_I} d^3r \tilde{v}_{\text{loc}}^I(\mathbf{r}) [\tilde{\rho}^{1,I}(\mathbf{r}) + \hat{\rho}^I(\mathbf{r})], \end{aligned} \quad (21)$$

$$\begin{aligned} E^1 = & \sum_{l,mn} \rho_{mn}^l \langle \Phi_m^{I,AE} | \frac{\mathbf{p}^2}{2} | \Phi_n^{I,AE} \rangle + \sum_I E_{\text{xc}}[\rho^{1,I} + \rho_c^I, \mathbf{m}^{1,I}] \\ & + \sum_I E_H[\rho^{1,I}] + \sum_I \int_{\Omega_I} d^3r v_{\text{loc}}^I(\mathbf{r}) \rho^{1,I}(\mathbf{r}), \end{aligned} \quad (22)$$

where the core charges  $\tilde{\rho}_c$  and  $\tilde{\rho}_c^I$  are defined as in Ref. 15 while we used the notation  $v_{\text{loc}}^I(\mathbf{r})$  for  $v_H(\rho_{Zc}^I)$  and  $\tilde{v}_{\text{loc}}^I(\mathbf{r})$  for  $v_H(\tilde{\rho}_{Zc}^I)$ ;  $\tilde{V}_{\text{loc}}(\mathbf{r})$  is equal to the sum  $\sum_I \tilde{v}_{\text{loc}}^I(\mathbf{r} - \mathbf{R}_I)$ . The minimization of this energy with respect to pseudo-wave-functions that obey to the orthogonality constraint  $\sum_\sigma \langle \tilde{\Psi}_{i,\sigma}^A | S | \tilde{\Psi}_{j,\sigma}^A \rangle = \delta_{i,j}$ , where the overlap matrix  $S$  is

$$S = 1 + \sum_{l,mn} q_{lmn}^l |\beta_m^I \rangle \langle \beta_n^I| \quad (23)$$

with  $q_{lmn}^l = \langle \Phi_m^{I,AE} | \Phi_n^{I,AE} \rangle - \langle \Phi_m^{I,PS} | \Phi_n^{I,PS} \rangle$ , yields the nonrelativistic PAW KS equations,

$$\sum_{\sigma_2} \left[ \frac{\mathbf{p}^2}{2} \delta^{\sigma_1, \sigma_2} + \int d^3r \tilde{V}_{\text{LOC}}^{\sigma_1, \sigma_2}(\mathbf{r}) \tilde{K}(\mathbf{r}) - \varepsilon_i S \delta^{\sigma_1, \sigma_2} + \sum_{l, mn} (D_{l, mn}^{1, \sigma_1, \sigma_2} - \tilde{D}_{l, mn}^{1, \sigma_1, \sigma_2}) |\beta_m^l\rangle \langle \beta_n^l| \right] |\tilde{\Psi}_{i, \sigma_2}\rangle = 0, \quad (24)$$

where

$$D_{l, mn}^{1, \sigma_1, \sigma_2} = \langle \Phi_m^{l, AE} | \frac{\mathbf{p}^2}{2} + V_{\text{LOC}}^{l, \sigma_1, \sigma_2} | \Phi_n^{l, AE} \rangle, \quad (25)$$

$$\tilde{D}_{l, mn}^{1, \sigma_1, \sigma_2} = \langle \Phi_m^{l, PS} | \frac{\mathbf{p}^2}{2} + \tilde{V}_{\text{LOC}}^{l, \sigma_1, \sigma_2} | \Phi_n^{l, PS} \rangle + \int_{\Omega_l} d^3r \hat{Q}_{mn}^l(\mathbf{r}) \tilde{V}_{\text{LOC}}^{l, \sigma_1, \sigma_2}(\mathbf{r}). \quad (26)$$

Notice that the coefficients of the nonlocal PP are spin dependent in this PAW formulation because they are calculated with the spin-dependent partial occupations. In the US-PPs case these coefficients are calculated in the nonmagnetic isolated atom and are spin independent. The function  $\tilde{K}(\mathbf{r})$  is defined in terms of the augmentation functions as

$$\tilde{K}(\mathbf{r}) = |\mathbf{r}\rangle \langle \mathbf{r}| + \sum_{l, mn} \hat{Q}_{mn}^l(\mathbf{r} - \mathbf{R}_l) |\beta_m^l\rangle \langle \beta_n^l|, \quad (27)$$

the potential  $V_{\text{LOC}}^{l, \sigma_1, \sigma_2}(\mathbf{r})$  is calculated with the local potential  $v_{\text{loc}}^l(\mathbf{r})$  and the charge and magnetization densities  $\rho^{1, l}(\mathbf{r})$  and  $\mathbf{m}^{1, l}(\mathbf{r})$ ,  $\tilde{V}_{\text{LOC}}^{l, \sigma_1, \sigma_2}(\mathbf{r})$  with  $\tilde{v}_{\text{loc}}^l(\mathbf{r})$ ,  $\tilde{\rho}^{1, l}(\mathbf{r}) + \hat{\rho}^l(\mathbf{r})$  and  $\tilde{\mathbf{m}}^{1, l}(\mathbf{r}) + \hat{\mathbf{m}}^l(\mathbf{r})$ , and  $\tilde{V}_{\text{LOC}}^{\sigma_1, \sigma_2}(\mathbf{r})$  with  $\tilde{V}_{\text{loc}}(\mathbf{r})$ ,  $\tilde{\rho}(\mathbf{r}) + \hat{\rho}(\mathbf{r})$ , and  $\tilde{\mathbf{m}}(\mathbf{r}) + \hat{\mathbf{m}}(\mathbf{r})$ .

Notice that, in practical applications, the present scheme is improved upon by generating the PAW data sets starting from the scalar relativistic equations in the isolated atom and therefore partially including relativistic effects.

#### IV. RSDFT WITHIN THE PAW METHOD

In the PAW approach to RSDFT, we want to rewrite the frozen-core total energy of a gas of  $N$  interacting electrons in the field of fixed ions at positions  $\mathbf{R}_l$  [Eq. (3)] as a functional of the four-component pseudo-wave-functions  $|\tilde{\Psi}_{i, \eta}\rangle$ . In the FR case, the partial waves and projectors are four-component spinors and the PAW mapping from pseudo to all-electron wave functions is

$$|\Psi_{i, \eta}\rangle = |\tilde{\Psi}_{i, \eta}\rangle + \sum_{l, m} \sum_{\eta_1} [|\Phi_{m, \eta}^{l, AE}\rangle - |\Phi_{m, \eta}^{l, PS}\rangle] \langle \beta_{m, \eta_1}^l | \tilde{\Psi}_{i, \eta_1}\rangle. \quad (28)$$

The all-electron partial waves are a product of radial functions, solutions of the atomic radial Dirac-type KS equations, and spin-angle functions dependent on the angular and spin variables (see Appendix B). Therefore, the index  $m$  is a shorthand notation for  $m = \{\tau, l, j, m_j\}$  that, in addition to  $\tau$  and  $l$  defined as in the nonrelativistic case ( $l$  is the orbital angular momentum of the large component), contains also  $j$

the total angular momentum and  $m_j$  its projection on a quantization axis. As in the nonrelativistic case, the pseudo- and all-electron partial waves coincide outside a given radius while inside the PAW spheres, the pseudo-partial-waves are obtained by a pseudization procedure starting from the all-electron partial waves (see Appendix A). The projectors are constructed after the pseudo-partial-waves with one of the usual recipes.<sup>14,24</sup> The difficulties encountered in the FR case have been discussed only for NC-PPs in Ref. 39. The PAW case is simpler to deal with because there is no NC constraint. There are several different options and a few of them are compared in Appendix A. When the partial waves and projectors are constructed as described in Appendix A, the following completeness relationship holds inside the spheres for sufficiently large  $N_\epsilon$  and  $l_{\text{max}}$ :

$$\sum_m |\Phi_{m, \eta_1}^{l, PS}\rangle \langle \beta_{m, \eta_2}^l| = \delta_{\eta_1, \eta_2} \quad (29)$$

when applied to any pseudo-wave-function. Consequently also the PAW mapping of the all-electron operators into pseudooperators Eq. (14) can be generalized in an obvious manner.

For instance, applying this PAW mapping to set the density matrix, we find its expression in terms of the pseudo-wave-functions.  $\rho_{\eta_1, \eta_2}(\mathbf{r})$  is the sum of three terms:  $\rho_{\eta_1, \eta_2}(\mathbf{r}) = \tilde{\rho}_{\eta_1, \eta_2}(\mathbf{r}) + \sum_I \rho_{\eta_1, \eta_2}^{1, I}(\mathbf{r}) - \sum_I \tilde{\rho}_{\eta_1, \eta_2}^{1, I}(\mathbf{r})$ , where

$$\tilde{\rho}_{\eta_1, \eta_2}(\mathbf{r}) = \sum_i \langle \tilde{\Psi}_{i, \eta_1} | \mathbf{r} \rangle \langle \mathbf{r} | \tilde{\Psi}_{i, \eta_2} \rangle, \quad (30)$$

$$\rho_{\eta_1, \eta_2}^{1, I}(\mathbf{r}) = \sum_{mn} \rho_{mn}^I \langle \Phi_{m, \eta_1}^{l, AE} | \mathbf{r} \rangle \langle \mathbf{r} | \Phi_{n, \eta_2}^{l, AE} \rangle, \quad (31)$$

$$\tilde{\rho}_{\eta_1, \eta_2}^{1, I}(\mathbf{r}) = \sum_{mn} \tilde{\rho}_{mn}^I \langle \Phi_{m, \eta_1}^{l, PS} | \mathbf{r} \rangle \langle \mathbf{r} | \Phi_{n, \eta_2}^{l, PS} \rangle, \quad (32)$$

where the partial occupations are

$$\rho_{mn}^I = \sum_{i, \eta_1, \eta_2} \langle \tilde{\Psi}_{i, \eta_1} | \beta_{m, \eta_1}^l \rangle \langle \beta_{n, \eta_2}^l | \tilde{\Psi}_{i, \eta_2} \rangle. \quad (33)$$

From the density matrix, the charge and magnetization densities are obtained readily as  $\rho(\mathbf{r}) = \sum_\eta \rho_{\eta, \eta}(\mathbf{r})$  and  $\mathbf{m}_k(\mathbf{r}) = \mu_B \sum_{\eta_1, \eta_2} \rho_{\eta_1, \eta_2}(\mathbf{r}) (\boldsymbol{\beta} \Sigma_k)^{\eta_1, \eta_2}$ .

As in the nonrelativistic case, we can add to the spin density calculated in real space a compensation spin density and write:  $\tilde{\rho}_{\eta_1, \eta_2}(\mathbf{r}) + \hat{\rho}_{\eta_1, \eta_2}(\mathbf{r}) = \sum_{i, \eta_3, \eta_4} \langle \tilde{\Psi}_{i, \eta_3} | \tilde{K}_{\eta_3, \eta_4}^{\eta_1, \eta_2}(\mathbf{r}) | \tilde{\Psi}_{i, \eta_4} \rangle$ , where the functions  $\tilde{K}_{\eta_3, \eta_4}^{\eta_1, \eta_2}(\mathbf{r})$  and the augmentation functions  $\hat{Q}_{mn, \eta_1, \eta_2}^l(\mathbf{r})$  which define the compensation spin density inside the spheres,  $[\hat{\rho}_{\eta_1, \eta_2}^{1, I}(\mathbf{r}) = \sum_{mn} \rho_{mn}^I \hat{Q}_{mn, \eta_1, \eta_2}^l(\mathbf{r})]$  are related by

$$\tilde{K}_{\eta_3, \eta_4}^{\eta_1, \eta_2}(\mathbf{r}) = |\mathbf{r}\rangle \langle \mathbf{r}| \delta^{\eta_1, \eta_3} \delta^{\eta_2, \eta_4} + \sum_{l, mn} \hat{Q}_{mn, \eta_1, \eta_2}^l(\mathbf{r} - \mathbf{R}_l) |\beta_{m, \eta_3}^l\rangle \langle \beta_{n, \eta_4}^l|. \quad (34)$$

The form of  $\hat{Q}_{mn, \eta_1, \eta_2}^l(\mathbf{r})$  is, to a certain extent, arbitrary. As long as the compensation charges  $\hat{\rho}^l(\mathbf{r})$

$= \sum_{mn} \sum_{\eta} \rho_{mn}^I \hat{Q}_{mn,\eta}^I(\mathbf{r})$  have the same multipole moments of  $\rho^{1,I}(\mathbf{r}) - \tilde{\rho}^{1,I}(\mathbf{r})$ ,  $\hat{Q}_{mn,\eta_1,\eta_2}^I(\mathbf{r})$  can be chosen so as to make  $\tilde{K}_{mn,\eta_1,\eta_2}^I(\mathbf{r})$  as smooth as possible. The simplest choice  $Q_{mn,\eta_1,\eta_2}^I(\mathbf{r}) = \langle \Phi_{m,\eta_1}^{I,AE} | \mathbf{r} | \Phi_{n,\eta_2}^{I,AE} \rangle - \langle \Phi_{m,\eta_1}^{I,PS} | \mathbf{r} | \Phi_{n,\eta_2}^{I,PS} \rangle$  leads to functions  $\tilde{K}_{mn,\eta_1,\eta_2}^I(\mathbf{r})$  that are too hard to expand in-plane waves and a pseudization method, like the one adopted in Ref. 15 or in Ref. 40, is necessary. In order not to slow down too much the exposition, we discuss the details of our approach in Appendix B. Here we just anticipate that the functions  $Q_{mn,\eta_1,\eta_2}^I(\mathbf{r})$  are replaced with smooth functions  $\hat{Q}_{mn,\eta_1,\eta_2}^I(\mathbf{r})$  whose Fourier expansion converges rapidly in-plane waves.

At this point, the charge density is separated as in the nonrelativistic case. Hence the Hartree and exchange and correlation energies can be calculated in the same way with terms evaluated on the real-space mesh and terms calculated inside the spheres.<sup>15</sup> Skipping the derivation that from this point onward becomes identical to that reported in Ref. 15, we write the FR frozen-core total energy as  $E_{\text{tot}} = \tilde{E} + E^1 - \tilde{E}^1$  with

$$\begin{aligned} \tilde{E} = & \sum_{i,\eta_1,\eta_2} \langle \tilde{\Psi}_{i,\eta_1} | T_D^{\eta_1,\eta_2} | \tilde{\Psi}_{i,\eta_2} \rangle + E_{\text{xc}}[\tilde{\rho} + \hat{\rho} + \tilde{\rho}_c, \tilde{\mathbf{m}} + \hat{\mathbf{m}}] \\ & + E_H[\tilde{\rho} + \hat{\rho}] + \int d^3r \tilde{V}_{\text{loc}}(\mathbf{r})[\tilde{\rho}(\mathbf{r}) + \hat{\rho}(\mathbf{r})] + U_{I,I}, \quad (35) \end{aligned}$$

$$\begin{aligned} \tilde{E}^1 = & \sum_{I,mn,\eta_1,\eta_2} \rho_{mn}^I \langle \Phi_{m,\eta_1}^{I,PS} | T_D^{\eta_1,\eta_2} | \Phi_{n,\eta_2}^{I,PS} \rangle + \sum_I E_{\text{xc}}[\tilde{\rho}^{1,I} + \hat{\rho}^I] \\ & + \tilde{\rho}_c^I, \tilde{\mathbf{m}}^{1,I} + \hat{\mathbf{m}}^{1,I}] + \sum_I E_H[\tilde{\rho}^{1,I} + \hat{\rho}^I] + \sum_I \int_{\Omega_I} d^3r \tilde{v}_{\text{loc}}^I(\mathbf{r}) \\ & \times [\tilde{\rho}^{1,I}(\mathbf{r}) + \hat{\rho}^I(\mathbf{r})], \quad (36) \end{aligned}$$

$$\begin{aligned} E^1 = & \sum_{I,mn,\eta_1,\eta_2} \rho_{mn}^I \langle \Phi_{m,\eta_1}^{I,AE} | T_D^{\eta_1,\eta_2} | \Phi_{n,\eta_2}^{I,AE} \rangle + \sum_I E_{\text{xc}}[\rho^{1,I} + \rho_c^I, \mathbf{m}^{1,I}] \\ & + \sum_I E_H[\rho^{1,I}] + \sum_I \int_{\Omega_I} d^3r v_{\text{loc}}^I(\mathbf{r}) \rho^{1,I}(\mathbf{r}), \quad (37) \end{aligned}$$

where the core charges  $\tilde{\rho}_c$  and  $\tilde{\rho}_c^I$  and the local potentials  $v_{\text{loc}}^I(\mathbf{r})$ ,  $\tilde{v}_{\text{loc}}^I(\mathbf{r})$ , and  $\tilde{V}_{\text{loc}}(\mathbf{r})$  are defined as in the nonrelativistic case.

The minimization of this energy with respect to pseudo-wave-functions that obey to the orthogonality constraint  $\sum_{\eta_1,\eta_2} \langle \tilde{\Psi}_{i,\eta_1} | S^{\eta_1,\eta_2} | \tilde{\Psi}_{j,\eta_2} \rangle = \delta_{i,j}$ , where the overlap matrix  $S$  is

$$S^{\eta_1,\eta_2} = \delta^{\eta_1,\eta_2} + \sum_{I,mn} q_{mn}^I |\beta_{m,\eta_1}^I\rangle \langle \beta_{n,\eta_2}^I| \quad (38)$$

with  $q_{mn}^I = \sum_{\eta} (\langle \Phi_{m,\eta}^{I,AE} | \Phi_{n,\eta}^{I,AE} \rangle - \langle \Phi_{m,\eta}^{I,PS} | \Phi_{n,\eta}^{I,PS} \rangle)$ , yields the PAW Dirac-type KS equations,

$$\begin{aligned} \sum_{\eta_2} \left[ T_D^{\eta_1,\eta_2} + \sum_{\eta_3,\eta_4} \int d^3r \tilde{V}_{\text{LOC}}^{\eta_3,\eta_4}(\mathbf{r}) \tilde{K}_{\eta_1,\eta_2}^{\eta_3,\eta_4}(\mathbf{r}) - \varepsilon_i S^{\eta_1,\eta_2} \right. \\ \left. + \sum_{I,mn} (D_{I,mn}^1 - \tilde{D}_{I,mn}^1) |\beta_{m,\eta_1}^I\rangle \langle \beta_{n,\eta_2}^I| \right] |\tilde{\Psi}_{i,\eta_2}\rangle = 0, \quad (39) \end{aligned}$$

where

$$D_{I,mn}^1 = \sum_{\eta_1,\eta_2} \langle \Phi_{m,\eta_1}^{I,AE} | T_D^{\eta_1,\eta_2} + V_{\text{LOC}}^{\eta_1,\eta_2} | \Phi_{n,\eta_2}^{I,AE} \rangle, \quad (40)$$

$$\begin{aligned} \tilde{D}_{I,mn}^1 = & \sum_{\eta_1,\eta_2} \langle \Phi_{m,\eta_1}^{I,PS} | T_D^{\eta_1,\eta_2} + \tilde{V}_{\text{LOC}}^{\eta_1,\eta_2} | \Phi_{n,\eta_2}^{I,PS} \rangle \\ & + \sum_{\eta_1,\eta_2} \int_{\Omega_I} d^3r \hat{Q}_{mn,\eta_1,\eta_2}^I(\mathbf{r}) \tilde{V}_{\text{LOC}}^{\eta_1,\eta_2}(\mathbf{r}). \quad (41) \end{aligned}$$

The potential  $V_{\text{LOC}}^{\eta_1,\eta_2}(\mathbf{r})$  is calculated with the local potential  $v_{\text{loc}}^I(\mathbf{r})$  and the charge and magnetization densities  $\rho^{1,I}(\mathbf{r})$  and  $\mathbf{m}^{1,I}(\mathbf{r})$ ,  $\tilde{V}_{\text{LOC}}^{\eta_1,\eta_2}(\mathbf{r})$  with  $\tilde{v}_{\text{loc}}^I(\mathbf{r})$ ,  $\tilde{\rho}^{1,I}(\mathbf{r}) + \hat{\rho}^I(\mathbf{r})$  and  $\tilde{\mathbf{m}}^{1,I}(\mathbf{r}) + \hat{\mathbf{m}}^I(\mathbf{r})$ , and  $\tilde{V}_{\text{LOC}}^{\eta_1,\eta_2}(\mathbf{r})$  with  $\tilde{V}_{\text{loc}}(\mathbf{r})$ ,  $\tilde{\rho}(\mathbf{r}) + \hat{\rho}(\mathbf{r})$ , and  $\tilde{\mathbf{m}}(\mathbf{r}) + \hat{\mathbf{m}}(\mathbf{r})$ .

Solving these equations, we get the FR PAW pseudo-wave-functions. From them the all-electron wave functions [Eq. (28)], the relativistic total energy [Eqs. (35)–(37)] and the RSDFT charge and magnetization densities [Eqs. (30)–(33)]. Ideally, these quantities are as accurate as the all-electron frozen-core results but, in practice, they are affected by the PAW data sets TEs. For instance, in atoms, PAW data sets can recover the frozen-core energies and the energy levels of atomic configurations close to the reference configuration with an accuracy of a few millirydberg. As highlighted in the next section, Eqs. (39)–(41) can be transformed into Pauli-type equations making errors comparable to the TEs or of order  $1/c^2$ . The TEs can be reduced by increasing the number of partial waves and projectors, but the intrinsic error of the Pauli-type equations cannot be smaller than  $1/c^2$ , so in the future the availability of increasingly larger computational resources might make the implementation and the solution of Eqs. (39)–(41) attractive but for our present purposes the Pauli-type equations are much less demanding computationally and, at the same time, of similar accuracy.

## V. FULLY RELATIVISTIC PAW VIA PAULI-TYPE EQUATIONS

### A. Kinetic energy

In this section we derive PAW Pauli-type KS equations that have an accuracy comparable to the PAW Dirac-type KS equations. We start by observing that, outside the PAW spheres, Pauli-type equations like those presented in Sec. II are a good approximation because in that region relativistic effects are small. Pauli-type equations introduce an error in the kinetic energy of order  $(v'/c)^2$  and, outside the spheres,  $v'$  is on the order of 1 a.u., often even lower about 0.5 a.u., so that  $(v'/c)^2 \approx 5 - 1 \times 10^{-5}$ , and this error is independent

from the nuclear charge  $Z_I$ . This observation allows us to write the relativistic kinetic energy in the form

$$E_{kin} = \sum_{i,\eta_1,\eta_2} \langle \Psi_{i,\eta_1} | T_D^{\eta_1,\eta_2} | \Psi_{i,\eta_2} \rangle_{\Omega} + \sum_{i,\sigma_1} \langle \Psi_{i,\sigma_1}^A | \frac{\mathbf{p}^2}{2} | \Psi_{i,\sigma_1}^A \rangle_{\bar{\Omega}}, \quad (42)$$

where the symbols  $\Omega$  and  $\bar{\Omega}$  indicate that the expectation values are to be calculated inside and outside the PAW spheres, respectively. Inside the spheres, we apply the PAW transformation of the operators while, outside the spheres, we simply replace the all-electron with pseudo-wave-functions because in that region they coincide. We obtain

$$\begin{aligned} E_{kin} = & \sum_{i,\eta_1,\eta_2} \langle \tilde{\Psi}_{i,\eta_1} | T_D^{\eta_1,\eta_2} | \tilde{\Psi}_{i,\eta_2} \rangle_{\Omega} + \sum_{i,\sigma_1} \langle \tilde{\Psi}_{i,\sigma_1}^A | \frac{\mathbf{p}^2}{2} | \tilde{\Psi}_{i,\sigma_1}^A \rangle_{\bar{\Omega}} \\ & + \sum_{I,mn,\eta_1,\eta_2} \rho_{mn}^I [\langle \Phi_{m,\eta_1}^{I,AE} | T_D^{\eta_1,\eta_2} | \Phi_{n,\eta_2}^{I,AE} \rangle_{\Omega} \\ & - \langle \Phi_{m,\eta_1}^{I,PS} | T_D^{\eta_1,\eta_2} | \Phi_{n,\eta_2}^{I,PS} \rangle_{\Omega}]. \end{aligned} \quad (43)$$

Now inside the spheres we can add a vanishing operator. The PAW method has the freedom to add a term written as<sup>14</sup>

$$B^{\eta_1,\eta_2} - \sum_{I,mn,\eta_3,\eta_4} |\beta_{m,\eta_1}^I\rangle \langle \Phi_{m,\eta_3}^{I,PS} | B^{\eta_3,\eta_4} | \Phi_{n,\eta_4}^{I,PS} \rangle_{\Omega} |\beta_{n,\eta_2}^I|. \quad (44)$$

For a complete set of pseudo-partial-waves and projectors, the expectation value of this term between pseudo-wave-functions vanishes identically whereas in practice it is comparable to the TE. Specifically, we take  $B=A-T_D$ , where  $A$  is a diagonal  $4 \times 4$  matrix that has the operator  $\mathbf{p}^2/2$  in the first two diagonal elements and is zero elsewhere. With this choice, Eq. (43) becomes

$$\begin{aligned} E_{kin} = & \sum_{i,\sigma_1} \langle \tilde{\Psi}_{i,\sigma_1}^A | \frac{\mathbf{p}^2}{2} | \tilde{\Psi}_{i,\sigma_1}^A \rangle \\ & + \sum_{I,mn} \rho_{mn}^I \left[ \sum_{\eta_1,\eta_2} \langle \Phi_{m,\eta_1}^{I,AE} | T_D^{\eta_1,\eta_2} | \Phi_{n,\eta_2}^{I,AE} \rangle_{\Omega} \right. \\ & \left. - \sum_{\sigma_1} \langle \Phi_{m,\sigma_1}^{I,PS,A} | \frac{\mathbf{p}^2}{2} | \Phi_{n,\sigma_1}^{I,PS,A} \rangle_{\Omega} \right]. \end{aligned} \quad (45)$$

Equation (45) shows that we can get the FR kinetic energy, applying  $\frac{\mathbf{p}^2}{2}$  to the pseudo-wave-functions. Outside the spheres because the Pauli-type equations hold [with an error of order  $(v'/c)^2$ ], inside the spheres because the difference between the Dirac kinetic energy and the nonrelativistic kinetic energy is compensated by the radial grid terms, where only the all-electron kinetic energy is evaluated using the Dirac operator. Using Pauli-type equations of higher order outside the spheres, for instance including mass-velocity, Darwin, and spin-orbit corrections,<sup>20</sup> we could reduce the errors in that region because we would have terms correct up to order  $(v'/c)^2$ , but in the other regions the accuracy is lower, because of the TEs and of the errors that we make in the following, so several other modifications are necessary to bring the overall accuracy to errors of order  $(v'/c)^3$ .

Notice that the kinetic energy in Eq. (45) is now dependent on the size of the PAW spheres  $\Omega$ , whereas the FR expression was independent from  $\Omega$ . Specifically, the terms  $\sum_{\eta_1,\eta_2} \langle \Phi_{m,\eta_1}^{I,AE} | T_D^{\eta_1,\eta_2} | \Phi_{n,\eta_2}^{I,AE} \rangle_{\Omega}$  diverge for unbound partial waves, a divergence that, in the FR case, is compensated by the terms  $\sum_{\eta_1,\eta_2} \langle \Phi_{m,\eta_1}^{I,PS} | T_D^{\eta_1,\eta_2} | \Phi_{n,\eta_2}^{I,PS} \rangle_{\Omega}$ . In Eq. (45) the divergence is compensated only for the large components not for the small ones. Now the integrals are finite because they are limited to the PAW spheres but at the same time they vary with the volume of the PAW spheres. This is unavoidable because the spheres introduce a separation between the region where the Dirac kinetic energy is dealt with exactly (modulo the TEs) and the region where there is an error of order  $(v'/c)^2$ . If the volumes of these two regions change, the kinetic energy changes as well but still with differences of order  $(v'/c)^2$ . Notice also that to obtain Eq. (45), we have not changed the FR PAW mapping between all-electron and pseudo-wave-functions, or changed the completeness relationship. We have only used the freedom of the PAW method to add an operator localized inside the spheres in the real-space mesh and to subtract the same operator inside the spheres.

## B. Removal of the small components of the pseudo-wave-functions

The small components of the pseudo-wave-functions, which are quantities of order  $1/c$ , cannot be obtained any longer through the minimization of the total energy that has now errors of order  $1/c^2$ . These small components are still present in the partial occupations [Eq. (33)], in the density matrix, and in the orthogonality constraints. To remove them everywhere, we have to make approximations that introduce errors comparable to the TEs or of order  $1/c^2$ , depending on which is the largest. The method illustrated in Appendix A introduces errors of order  $v_1^4/c^2$ , where  $v_1^4$  is never larger than about 10 a.u.. This error can be reduced or even canceled (see A) if it will become larger than the TEs but so far it is a small error and we have kept it in the formalism.

In general, the shapes of the pseudo-wave-functions inside the PAW spheres are arbitrary. They must match continuously the all-electron wave functions at the border of the PAW spheres but they have not the oscillations of the all-electron wave functions. At the border of the spheres, the small components of the all-electron wave functions are of order  $(v'/c)$  independently from the nuclear charge  $Z_I$  and the small components of the pseudo-wave-functions can be kept everywhere of order  $v_1/c$  (here  $v_1$  varies with the state and is also position dependent but usually is smaller than 1 or 2 a.u.). In Appendix A, we show that the small components of the projectors can be defined so as to be of order  $v_1^3/c$  hence the product  $\sum_{\eta} \langle \tilde{\Psi}_{i,\eta} | \beta_{m,\eta}^I \rangle$  in Eq. (33) is equal to  $\sum_{\sigma} \langle \tilde{\Psi}_{i,\sigma}^A | \beta_{m,\sigma}^{I,A} \rangle$  up to a term of order  $v_1^4/c^2$  that can be neglected thus removing from the partial occupations the small components of the pseudo-wave-functions.

Let us now consider the density matrix [Eqs. (30)–(33)]. To remove the small components of the pseudo-wave-functions from its expression, we use again the possibility offered by the PAW method to add a vanishing term inside the spheres [see Eq. (44)] and take as  $B^{\eta_1,\eta_2}$  a diagonal op-

erator with  $-|\mathbf{r}\rangle\langle\mathbf{r}|$  in the third and fourth diagonal elements and zero elsewhere. After a few steps similar to those illustrated for the kinetic energy we get

$$\rho_{\sigma_1, \sigma_2}(\mathbf{r}) = \sum_i \langle \tilde{\Psi}_{i, \sigma_1}^A | \mathbf{r} \rangle \langle \tilde{\Psi}_{i, \sigma_2}^A | \mathbf{r} \rangle + \sum_{I, mn} \rho_{mn}^I [\langle \Phi_{m, \sigma_1}^{I, AE} | \mathbf{r} \rangle \langle \Phi_{n, \sigma_2}^{I, AE} | \mathbf{r} \rangle - \langle \Phi_{m, \sigma_1}^{I, PS, A} | \mathbf{r} \rangle \langle \Phi_{n, \sigma_2}^{I, PS, A} | \mathbf{r} \rangle] \quad (46)$$

for the first upper  $2 \times 2$  block and

$$\rho_{\eta_1, \eta_2}(\mathbf{r}) = \sum_{I, mn} \rho_{mn}^I \langle \Phi_{m, \eta_1}^{I, AE} | \mathbf{r} \rangle \langle \Phi_{n, \eta_2}^{I, AE} | \mathbf{r} \rangle \quad (47)$$

for the other blocks. Equation (46) tells us that the large components of the pseudo-wave-functions suffice to calculate the density matrix on the real-space mesh as far as only the large components of the pseudo-partial-waves are used inside the spheres to get  $\tilde{\rho}_{\eta_1, \eta_2}^{1, I}$ . Only the all-electron-density matrix inside the spheres ( $\rho_{\eta_1, \eta_2}^{1, I}$ ) needs both the large and the small components of the all-electron partial waves. In Eq. (46), we have neglected the small components of the pseudo-wave-functions outside the spheres with an error of order  $(v'/c)^2$ . For example, in a Pt atom the charge density due to these terms is about  $10^{-5}$  electrons, at least two orders of magnitude smaller than the charge due to the small components of the all-electron valence wave functions.

The pseudo-wave-functions obey to orthogonality constraints [Eq. (38)], which depend on both the large and the small components. We can now transform this constraint by adding, inside the spheres a vanishing term as in Eq. (44) with  $B^{\eta_1, \eta_2}$  equal to a diagonal operator with  $-1$  in the third and fourth diagonal elements and zero elsewhere. By this method, we obtain the first upper  $2 \times 2$  block of the overlap matrix,

$$S^{\sigma_1, \sigma_2} = \delta^{\sigma_1, \sigma_2} + \sum_{I, mn} |\beta_{m, \sigma_1}^{I, A}\rangle \left[ \sum_{\eta_1} \langle \Phi_{m, \eta_1}^{I, AE} | \Phi_{n, \eta_1}^{I, AE} \rangle_{\Omega} - \sum_{\sigma_3} \langle \Phi_{m, \sigma_3}^{I, PS, A} | \Phi_{n, \sigma_3}^{I, PS, A} \rangle_{\Omega} \right] \langle \beta_{n, \sigma_2}^{I, A} |. \quad (48)$$

The other blocks contribute to the orthogonality constraint with terms of order  $v_1^4/c^2$  or smaller and can be neglected. Equation (48) can be obtained also starting from the spin-density, Eq. (46), and requiring the integral of the charge density to be equal to the number of electrons.

### C. Total energy and PAW Pauli-type KS equations

We can now define the charge densities inside the spheres,  $\rho^{1, I}(\mathbf{r})$  as in the previous section, and  $\tilde{\rho}^{1, I}(\mathbf{r}) = \sum_{mn} \sum_{\sigma} \rho_{mn}^I \langle \Phi_{m, \sigma}^{I, PS, A} | \mathbf{r} \rangle \langle \Phi_{n, \sigma}^{I, PS, A} | \mathbf{r} \rangle$ . Introducing a compensation charge  $\hat{\rho}^I(\mathbf{r})$  with the same multipole moments of  $\rho^{1, I}(\mathbf{r}) - \tilde{\rho}^{1, I}(\mathbf{r})$  as in the FR case, we can proceed to the separation of the Hartree and exchange and correlation energies into terms calculated in the real-space mesh and terms calculated inside the spheres. We get the frozen-core total energy in the form  $E_{\text{tot}} = \tilde{E} + E^1 - \tilde{E}^1$ , where  $E^1$  is given by Eq. (37) while

$$\tilde{E} = \sum_{i, \sigma} \langle \tilde{\Psi}_{i, \sigma}^A | \frac{\mathbf{p}^2}{2} | \tilde{\Psi}_{i, \sigma}^A \rangle + E_{\text{xc}}[\tilde{\rho} + \hat{\rho} + \tilde{\rho}_c, \tilde{\mathbf{m}} + \hat{\mathbf{m}}] + E_H[\tilde{\rho} + \hat{\rho}] + \int d^3r \tilde{V}_{\text{loc}}(\mathbf{r})[\tilde{\rho}(\mathbf{r}) + \hat{\rho}(\mathbf{r})] + U_{I, I}, \quad (49)$$

$$\tilde{E}^1 = \sum_{I, mn, \sigma} \rho_{mn}^I \langle \Phi_{m, \sigma}^{I, PS, A} | \frac{\mathbf{p}^2}{2} | \Phi_{n, \sigma}^{I, PS, A} \rangle + \sum_I E_{\text{xc}}[\tilde{\rho}^{1, I} + \hat{\rho}^I + \tilde{\rho}_c^I, \tilde{\mathbf{m}}^I + \hat{\mathbf{m}}^I] + \sum_I E_H[\tilde{\rho}^{1, I} + \hat{\rho}^I] + \sum_I \int_{\Omega_I} d^3r \tilde{v}_{\text{loc}}^I(\mathbf{r})[\tilde{\rho}^{1, I}(\mathbf{r}) + \hat{\rho}^I(\mathbf{r})]. \quad (50)$$

The minimization of the total energy with respect to wave functions that obey the orthogonality constraints [Eq. (48)] leads to the following expression for the Pauli-type PAW KS equation:

$$\sum_{\sigma_2} \left[ \frac{\mathbf{p}^2}{2} \delta^{\sigma_1, \sigma_2} + \sum_{\eta_1, \eta_2} \int d^3r \tilde{V}_{\text{LOC}}^{\eta_1, \eta_2}(\mathbf{r}) \tilde{K}(\mathbf{r})^{\eta_1, \eta_2} - \varepsilon_i S^{\sigma_1, \sigma_2} + \sum_{I, mn} (D_{I, mn}^1 - \tilde{D}_{I, mn}^1) |\beta_{m, \sigma_1}^{I, A}\rangle \langle \beta_{n, \sigma_2}^{I, A}| \right] | \tilde{\Psi}_{i, \sigma_2}^A \rangle = 0, \quad (51)$$

where

$$D_{I, mn}^1 = \sum_{\eta_1, \eta_2} \langle \Phi_{m, \eta_1}^{I, AE} | T_D^{\eta_1, \eta_2} + V_{\text{LOC}}^{\eta_1, \eta_2} | \Phi_{n, \eta_2}^{I, AE} \rangle, \quad (52)$$

$$\tilde{D}_{I, mn}^1 = \sum_{\sigma_1, \sigma_2} \langle \Phi_{m, \sigma_1}^{I, PS, A} | \frac{\mathbf{p}^2}{2} \delta^{\sigma_1, \sigma_2} + \tilde{V}_{\text{LOC}}^{\sigma_1, \sigma_2} | \Phi_{n, \sigma_2}^{I, PS, A} \rangle + \sum_{\eta_1, \eta_2} \int_{\Omega_I} d^3r \hat{Q}_{mn, \eta_1, \eta_2}^I(\mathbf{r}) \tilde{V}_{\text{LOC}}^{\eta_1, \eta_2}(\mathbf{r}). \quad (53)$$

These Pauli-type KS equations resemble the FR US-PPs equations and we can exploit this similarity to write them as the nonrelativistic PAW equations, following the approach of Refs. 27 and 28. The projectors depend on spin through the spin-angle functions; they can be written in terms of spherical harmonics, transferring the spin index to the nonlocal PP coefficients as shown in Ref. 27 for FR US-PPs. The sums over  $\eta$  that appear in Eqs. (51)–(53) can be carried out analytically (see Appendix B) so that the angular and spin dependence can be dealt with as in the US-PPs case with minor changes in the calculation of  $D_{I, mn}^1$ . After these transformations, the Hamiltonian and the total energy become formally identical to the nonrelativistic ones, and the Hellmann-Feynman forces as well as density functional perturbation theory can be written as in Refs. 17 and 28.

Kleinman's<sup>25</sup> observation that a NC-PP tailored on the solutions of a Dirac-type equation could yield the FR results with errors of order  $1/c^2$  is implicit in our method. However, in the NC case there is no well established procedure to deal with the charge density of the small components of the valence all-electron wave functions. If the small components are neglected, the large components are not normalized. For instance, in a Pt atom, the valence charge of the small components of the  $5d_{3/2}$  and  $5d_{5/2}$  states, which are occupied by

TABLE I. Comparison of the PBE energy eigenvalues and of the total energies calculated by FR PAW data sets and by solving an all-electron atomic Dirac-type equation for a few atomic configurations of Fe. The reported eigenvalues are the all-electron ones (in Ry and without the minus sign). In parenthesis the difference (in mRy) between the all-electron and the PP results. The latter have been obtained by the FR PAW Pauli-type method. The PP eigenvalue is the algebraic sum of the all-electron eigenvalue and the number in parenthesis. The total-energy difference ( $\Delta E$  in Ry) is given with respect to the reference configuration. In square bracket we report the difference of the eigenvalues found by solving the all-electron Dirac-Kohn-Sham equations and the frozen-core all-electron Dirac-Kohn-Sham equations with the same sign convention.

Fe ( $3s^2 3p^6$ )	$3d_{3/2}^4 3d_{5/2}^3 4s_{1/2}$	$3d_{3/2}^4 3d_{5/2}^2 4s_{1/2} 4p_{1/2}$	$3d_{3/2}^4 3d_{5/2}^2 4s_{1/2}$
$3d_{3/2}$	0.2848 (-0.4)	0.6774 (-0.2)	1.1772 (-0.3)
$3d_{5/2}$	0.2748 (-0.4)	0.6662 (-0.2)	1.1659 (-0.3)
$4s_{1/2}$	0.3125 (0.4)	0.4655 (0.0)	0.9057 (0.1)
$4p_{1/2}$	0.0652 (0.1)	0.1571 (0.0)	0.5431 (0.0)
$4p_{3/2}$	0.0630 (0.1)	0.1533 (0.0)	0.5372 (0.0)
$\Delta E$	-0.0523 (-0.6)	0.2990 (0.0)	0.6413 (0.0)
Fe	$3d_{3/2}^4 3d_{5/2}^3 4s_{1/2}$	$3d_{3/2}^4 3d_{5/2}^2 4s_{1/2} 4p_{1/2}$	$3d_{3/2}^4 3d_{5/2}^2 4s_{1/2}$
$3d_{3/2}$	0.2848 (-3.6) [-3.4]	0.6774 (4.4) [4.6]	1.1772 (4.0) [4.1]
$3d_{5/2}$	0.2748 (-3.5) [-3.4]	0.6662 (4.4) [4.5]	1.1659 (4.0) [4.1]
$4s_{1/2}$	0.3125 (1.9) [1.7]	0.4655 (-0.2) [-0.1]	0.9057 (0.0) [0.0]
$4p_{1/2}$	0.0652 (0.9) [0.8]	0.1571 (-0.2) [-0.2]	0.5431 (0.0) [0.0]
$4p_{3/2}$	0.0630 (0.9) [0.8]	0.1533 (-0.2) [-0.2]	0.5372 (0.0) [-0.1]
$\Delta E$	0.0156 (-2.3) [-2.1]	0.3356 (-0.6) [-0.6]	0.6779 (0.5) [0.5]

ten electrons, is about  $2 \times 10^{-3}$  electrons so the missing norm of each state is about  $2 \times 10^{-4}$ . This error is small but has to be corrected in some way. In Ref. 27, we normalized the large components of the bound all-electron partial waves before applying the pseudization procedure obtaining FR US-PPs with good transferability properties. Alternatively, the radial Dirac-type equation can be inverted accounting for the presence of the small components, as suggested in Ref. 39. Within the PAW formalism, the correct charge is recovered from the all-electron partial waves that are calculated exactly. In the Pauli-type case, we still have an error of order  $1/c^2$  due the missing norm of the small components of the pseudo-wave-functions outside the PAW spheres. In the calculations presented below this error has been compensated normalizing both the large and the small components of the bound all-electron partial waves. The missing norm is however small. For instance, in Pt, it turns out to be about  $10^{-6}$  per state.

## VI. APPLICATIONS

The PAW Pauli-type equations [Eq. (51)] have been implemented in the QUANTUM ESPRESSO package,<sup>41</sup> and here we present a few results obtained with this feature. The present method, specialized to FR US-PPs, was applied in Refs. 27–32. That implementation was the starting point of the present PAW extension (see Appendix B). As applications, we compare the PAW electronic band structures of fcc-Pt and fcc-Au and of the ferromagnetic bcc-Fe with published results. The local-density approximation (LDA) (Ref. 42) is used for the exchange and correlation energies in

fcc-Pt and fcc-Au and the spin-polarized generalized gradient approximation of Perdew-Burke and Ernzerhof (PBE) (Ref. 43) is used for bcc-Fe. No relativistic correction has been included in the exchange and correlation functionals. The PAW data sets of Fe, Pt, and Au are described in the note.<sup>44</sup> For each element, we considered two PAW data sets, one including semicore states ( $3s$  and  $3p$  for Fe,  $5s$  and  $5p$  for Pt and Au) and one without semicore states. The kinetic-energy cutoffs for the wave functions of Fe (Pt) [Au] are 45 Ry (40 Ry) [35 Ry] for the data sets without semicore states and 75 Ry (60 Ry) [80 Ry] for data sets with semicore states. The cutoffs for the charge density are always 300 Ry except for Fe with semicore states for which we used 400 Ry. In bcc-Fe (fcc-Pt and fcc-Au), we sampled the BZ by a  $24 \times 24 \times 24$  ( $16 \times 16 \times 16$ ) uniform  $\mathbf{k}$ -point grid and a smearing parameter  $\sigma=0.02$  Ry.

We start by considering the TE of the FR PAW data sets. We report in Tables I–III the energy levels of a few atomic configurations and the difference between their total energy and the energy of the reference configuration.<sup>44</sup> The magnitude of the TEs, indicated in parenthesis, is of a few millirydbergs for the data sets without semicore states and of fractions of millirydberg for those with semicore states. The larger TEs found in the former case can be attributed to the frozen-core approximation because they are similar to the errors reported in square brackets that are obtained as the difference between the all-electron eigenvalues and the eigenvalues of an all-electron calculation in which the core states are kept frozen in the reference configuration. Finally, notice that the values of the TEs found in Tables I–III are similar to the typical TEs of SR data sets and are larger than  $1/c^2$ .

TABLE II. As in Table I for Pt with the LDA functional.

Pt ( $5s^25p^6$ )	$5d_{3/2}^4 5d_{5/2}^6 6s_{1/2}^0$	$5d_{3/2}^4 5d_{5/2}^4 6s_{1/2}^2$	$5d_{3/2}^4 5d_{5/2}^4 6s_{1/2}$
$5d_{3/2}$	0.4066 (0.0)	0.6639 (0.2)	1.2896 (0.2)
$5d_{5/2}$	0.3143 (0.0)	0.5596 (0.1)	1.1823 (0.2)
$6s_{1/2}$	0.3853 (0.1)	0.4970 (0.0)	1.0508 (0.0)
$6p_{1/2}$	0.0734 (0.0)	0.1322 (0.0)	0.6135 (0.0)
$6p_{3/2}$	0.0407 (0.0)	0.0835 (0.0)	0.5301 (0.0)
$\Delta E$	0.0415 (0.0)	0.0254 (-0.1)	0.7944 (0.1)
Pt	$5d_{3/2}^4 5d_{5/2}^6 6s_{1/2}^0$	$5d_{3/2}^4 5d_{5/2}^4 6s_{1/2}^2$	$5d_{3/2}^4 5d_{5/2}^4 6s_{1/2}$
$5d_{3/2}$	0.4066 (-1.1) [-1.1]	0.6639 (3.1) [3.2]	1.2896 (4.0) [3.9]
$5d_{5/2}$	0.3143 (-0.8) [-0.8]	0.5596 (2.7) [2.8]	1.1823 (3.6) [3.6]
$6s_{1/2}$	0.3853 (0.9) [0.8]	0.4970 (-0.2) [-0.2]	1.0508 (0.3) [0.4]
$6p_{1/2}$	0.0734 (0.7) [0.6]	0.1322 (-0.3) [-0.3]	0.6135 (0.1) [0.1]
$6p_{3/2}$	0.0407 (0.6) [0.6]	0.0835 (-0.2) [-0.3]	0.5301 (0.3) [0.5]
$\Delta E$	0.0415 (-0.9) [-0.9]	0.0254 (-1.4) [-1.3]	0.7944 (-1.4) [-1.4]

The theoretical lattice constants and bulk moduli of the three metals considered in this work are reported in Table IV and compared with experiment and with previous FR calculations.<sup>11,27,45</sup> In Ref. 11 the all-electron Dirac-type equations are solved, in Ref. 45 the all-electron Pauli-type equations are solved and spin orbit is included while in Ref. 27 FR US-PPs are used. In fcc-Pt and fcc-Au, PAW data sets with semicore states give theoretical lattice constants that agree to better than 0.01 a.u. with the all-electron results of Ref. 11. Slightly larger lattice constants result instead neglecting semicore states. The influence of semicore states on the bulk moduli is weaker, and there is also a negligible effect on the structural and magnetic properties of bcc-Fe. For comparison, in Table IV we report the structural properties obtained with SR PAW data sets constructed with the same parameters. As in Ref. 27, we still find that the inclusion of spin-orbit coupling has only a marginal effect on the

lattice constants, smaller than that of semicore states, but has a detectable effect on the bulk moduli. Surprisingly, the same applies also to bcc-Fe, where spin-orbit effects are expected to be small. The reason for this is presently unclear and will require further investigations. We notice only that the sign of the spin-orbit effects on the bulk modulus is material dependent, with a decrease in bcc-Fe and fcc-Pt and an increase in fcc-Au.

In Table V, we report the electronic band structures of fcc-Pt and fcc-Au in a few high-symmetry points of the Brillouin zone and compare the results with those obtained by the FR US-PPs in Ref. 27 and by the solution of the Dirac-type KS equations in Ref. 11. All results have been obtained at the same lattice constant used in Ref. 11. In Ref. 27 we used a  $8 \times 8 \times 8$   $\mathbf{k}$ -point mesh as in Ref. 11, while here we are using a  $16 \times 16 \times 16$  mesh, to obtain more converged results. Although the US-PPs of Ref. 27 and the present PAW

TABLE III. As in Table I for Au with the LDA functional.

Au ( $5s^25p^6$ )	$5d_{3/2}^4 5d_{5/2}^5 6s_{1/2}^2$	$5d_{3/2}^4 5d_{5/2}^5 6s_{1/2}$	$5d_{3/2}^4 5d_{5/2}^4 6s_{1/2}^2$
$5d_{3/2}$	0.7434 (0.2)	1.3887 (0.1)	1.5674 (0.5)
$5d_{5/2}$	0.6238 (0.1)	1.2663 (0.1)	1.4384 (0.4)
$6s_{1/2}$	0.5114 (0.1)	1.0814 (0.0)	1.1625 (0.0)
$6p_{1/2}$	0.1307 (-0.1)	0.6249 (-0.1)	0.6805 (0.4)
$6p_{3/2}$	0.0793 (-0.1)	0.5358 (-0.1)	0.5816 (0.2)
$\Delta E$	0.0715 (0.1)	0.8628 (0.0)	1.0924 (0.3)
Au	$5d_{3/2}^4 5d_{5/2}^5 6s_{1/2}^2$	$5d_{3/2}^4 5d_{5/2}^5 6s_{1/2}$	$5d_{3/2}^4 5d_{5/2}^4 6s_{1/2}^0$
$5d_{3/2}$	0.7434 (3.2) [3.2]	1.3887 (4.0) [4.0]	1.2199 (-0.3) [-0.3]
$5d_{5/2}$	0.6238 (2.8) [2.8]	1.2663 (3.5) [3.5]	1.1038 (-0.3) [-0.2]
$6s_{1/2}$	0.5114 (-0.2) [-0.2]	1.0814 (0.3) [0.3]	1.0004 (0.2) [0.2]
$6p_{1/2}$	0.1307 (-0.3) [-0.3]	0.6249 (0.1) [0.1]	0.5668 (0.2) [0.2]
$6p_{3/2}$	0.0793 (-0.2) [-0.2]	0.5358 (0.3) [0.1]	0.4863 (0.2) [0.1]
$\Delta E$	0.0715 (-1.4) [-1.3]	0.8628 (-1.5) [-1.4]	0.7196 (-0.1) [-0.1]

TABLE IV. Theoretical lattice constants ( $a_0$ ) and bulk moduli ( $B_0$ ) of the systems studied in this work compared with previous calculations and with experiments. For ferromagnetic bcc-Fe, we report also the magnetic moment  $\mu$  at the equilibrium lattice constant.

	Fe (PBE)			Pt (LDA)		Au (LDA)	
	$a_0$ (a.u.)	$B_0$ (GPa)	$\mu$ ( $\mu_B$ )	$a_0$ (a.u.)	$B_0$ (GPa)	$a_0$ (a.u.)	$B_0$ (GPa)
No semicore (FR)	5.358	189	2.17	7.403	301	7.666	199
Semicore (FR)	5.360	189	2.16	7.372	300	7.633	200
No semicore (SR)	5.355	196	2.17	7.396	306	7.681	192
Semicore (SR)	5.357	196	2.17	7.365	305	7.648	194
Reference 11 (FR)				7.370	297	7.637	195
Reference 45 (FR)				7.386		7.648	
Reference 27 (FR US-PPs)				7.40	292	7.640	198
Expt.	5.42 <sup>a</sup>	168 <sup>a</sup>	2.22 <sup>a</sup>	7.40 <sup>b</sup> , 7.394 <sup>c</sup>	283 <sup>b</sup>	7.67 <sup>b</sup> , 7.676 <sup>c</sup>	173 <sup>b</sup>

<sup>a</sup>Reference 46.

<sup>b</sup>Extrapolated at  $T=0$ . Reference 47.

<sup>c</sup>Extrapolated at  $T=0$ . Reference 45.

data sets have been generated with quite different recipes, the agreement between the two band structures is good with errors mostly below 0.03 eV. The average difference in the fcc-Pt case is of about 0.01 eV. In fcc-Au, the average difference appears larger (about 0.07 eV) but this is due to the different  $\mathbf{k}$ -point sampling. With a  $8 \times 8 \times 8$  mesh, the difference is below 0.03 eV. When compared to the all-electron results of Ref. 11, the PAW data sets are nearly equivalent to the US-PPs, both giving average absolute differences of about 0.06 eV for fcc-Pt. For fcc-Au, the average absolute differences are 0.04 eV and 0.06 eV in PAW and US-PPs case, respectively, but the smaller PAW error is only due to the different  $\mathbf{k}$ -point samplings. Since the numerical values of Ref. 11 have been extracted from a figure and have some uncertainty, and have been obtained with a slightly different parametrization of the exchange and correlation energies, we cannot give too much meaning to the tiny differences between the two methods and both appear reasonably good. Finally, we notice that although the PAW data sets without semicore states have a worse transferability in the atomic tests, they are acceptable to calculate the electronic band structures. The energy differences between the data sets with and without semicore states are mostly within 0.01 eV.

The electronic bands of ferromagnetic bcc-Fe close to the Fermi energy, at the experimental lattice constant ( $a_0 = 5.42$  a.u.), are reported in Fig. 1.<sup>48</sup> We show the bands obtained with data set without semicore states but the results are almost independent from the data set used, the largest differences being of about 0.02 eV. In Fig. 1, we show the bands along  $\Gamma$ - $H$  [ $H=(1,0,0)$  in units of  $\frac{2\pi}{a_0}$ ] and  $\Gamma$ - $H'$  [ $H'=(0,0,1)$ ]. The magnetization vector is, in all points, parallel to the  $z$  axis, so in the first line, the  $\mathbf{k}$  vectors are perpendicular to the magnetization, whereas in the second line they are parallel to the magnetization. In Fig. 1, we have indicated with different line types and colors bands of different symmetry with respect to the operations that do not contain time reversal.<sup>49</sup> Along the  $\Gamma$ - $H$  direction, the relevant symmetry group is  $C_s$ , the mirror plane containing the mag-

netization vector and the  $\mathbf{k}$  points, and the states are divided among the  $\Gamma_3$  and  $\Gamma_4$  representations. Along  $\Gamma$ - $H'$  the relevant symmetry group is  $C_4$  with the rotation axis parallel to the magnetization. There are states of four different symmetries indicated with  $\Gamma_5$ ,  $\Gamma_6$ ,  $\Gamma_7$ , and  $\Gamma_8$ . At the points  $\Gamma$ ,  $H$ , and  $H'$  the symmetry group becomes  $C_{4h}$ . All the bands shown in Fig. 1 are even with respect to inversion and the representations becomes  $\Gamma_5^+$ ,  $\Gamma_6^+$ ,  $\Gamma_7^+$ , and  $\Gamma_8^+$ . Similar bands calculated using a NC-PP and an all-electron code were presented in Refs. 33 and 34. Both calculations agree quite well with each other and with the present result and also the all-electron magnetic moment reported in Ref. 34 (2.226  $\mu_B$ ) agrees with our value.

In conclusion, we have written the PAW Dirac-type equations of RSDFT and we have transformed these equations into Pauli-type equations making errors of order  $1/c^2$  or comparable to the TEs. In heavy atoms, these errors are much smaller than the errors of order  $(Z_1/c)^3$  of the second-order Taylor expansions of the Dirac-type equation. We solved the Pauli-type equations for fcc-Pt, fcc-Au, and ferromagnetic bcc-Fe and we showed that the PAW band structures match the band structures of the all-electron Dirac-type equations. The FR US-PPs (Ref. 27) are a further approximation of the present scheme in which, inside the PAW spheres, the partial occupations are linearized about the atomic partial occupations so that the bare coefficients of the nonlocal PP can be calculated in the isolated atoms. The FR US-PPs turn out to give results that compare well with the present FR PAW results.

#### ACKNOWLEDGMENTS

I thank G. Sclauzero for useful discussions. This work was sponsored by INFN/CNR ‘‘Iniziativa trasversale calcolo parallelo.’’ The calculations have been done on the SISSA Linux cluster and at CINECA in Bologna.

#### APPENDIX A: THE RELATIVISTIC PAW DATA SET

Partial waves and projectors are calculated in a nonmagnetic, isolated atom. The magnitude of the small components

TABLE V. The energy eigenvalues (in eV and at the lattice constant indicated in the first row) of fcc-Pt and fcc-Au at high-symmetry points are compared with results obtained by four-component relativistic Dirac-type equations (Ref. 11) or by FR US-PPs (Ref. 27). The Fermi energy is at zero. The reported values refer to PAW data sets without semicore states while in parenthesis we report the difference, on the last digit, obtained with semicore states.

	Pt (this work)	Pt (Ref. 27)	Pt (Ref. 11)	Au (this work)	Au (Ref. 27)	Au (Ref. 11)
$a_0$ (a.u.)	7.414	7.414	7.414	7.707	7.707	7.707
$\Gamma$	-10.38 (-1)	-10.39	-10.35	-10.07(1)	-10.01	-9.95
	-4.35 (0)	-4.35	-4.24	-5.41 (-1)	-5.35	-5.32
	-3.36 (0)	-3.35	-3.28	-4.21 (-1)	-4.14	-4.14
	-1.51 (0)	-1.52	-1.48	-2.97 (-1)	-2.92	-2.96
X	-7.23 (0)	-7.22	-7.10	-7.30 (0)	-7.23	-7.14
	-6.79 (0)	-6.78	-6.70	-7.01 (0)	-6.94	-6.95
	-0.24 (0)	-0.25	-0.20	-2.27 (-1)	-2.22	-2.27
	0.06 (1)	0.05	0.04	-2.06 (-1)	-2.01	-2.07
W				-1.03 (-1)	-0.98	-1.03
	-5.84 (0)	-5.84	-5.72	-6.27 (0)	-6.21	-6.16
	-4.88 (0)	-4.89	-4.83	-5.69 (0)	-5.63	-5.67
	-4.63 (0)	-4.62	-4.58	-5.12 (0)	-5.05	-5.08
L	-1.95 (2)	-1.93	-1.87	-3.21 (1)	-3.15	-3.20
				-1.61 (-1)	-1.56	-1.62
	-7.50 (-1)	-7.48	-7.44	-7.56 (0)	-7.48	-7.53
	-4.50 (0)	-4.49	-4.43	-5.52 (-1)	-5.46	-5.52
K	-3.49 (0)	-3.49	-3.45	-4.33 (0)	-4.28	-4.33
	-0.72 (-1)	-0.74	-0.79	-2.32 (0)	-2.27	-2.37
	-0.32 (-1)	-0.33	-0.30	-1.60 (-1)	-1.55	-1.62
				-1.23 (1)	-1.10	-1.23
K	-6.43 (1)	-6.42	-6.40	-6.72 (0)	-6.66	-6.70
	-5.66 (-1)	-5.66	-5.57	-6.14 (-1)	-6.07	-6.11
	-3.07 (0)	-3.08	-3.00	-4.03 (0)	-3.95	-4.04
	-1.39 (0)	-1.38	-1.38	-2.97 (0)	-2.92	-3.00
	-0.10 (0)	-0.10	-0.10	-1.92 (0)	-1.86	-1.97

of the pseudo-partial-waves and of the projectors varies with the construction recipe.  $\Phi_m^{IAE}(\mathbf{r})$  depends on the angular and spin variables through spin-angle functions (see below), whereas the radial components are the solutions of the radial Dirac-type equations. For a given  $\tau$  and  $\kappa$ , from the solutions of the coupled equations,

$$-c \left( \frac{d}{dr} + \frac{\kappa}{r} \right) \mathcal{Q}_{\tau,\kappa}(r) + [V_{\text{eff}}(r) - \varepsilon_{\tau,\kappa}] \mathcal{P}_{\tau,\kappa}(r) = 0, \quad (\text{A1})$$

$$c \left( \frac{d}{dr} - \frac{\kappa}{r} \right) \mathcal{P}_{\tau,\kappa}(r) + [V_{\text{eff}}(r) - \varepsilon_{\tau,\kappa} - 2c^2] \mathcal{Q}_{\tau,\kappa}(r) = 0, \quad (\text{A2})$$

the large and small radial components of  $\Phi_m^{IAE}(\mathbf{r})$  are  $\mathcal{P}_{\tau,\kappa}(r)/r$  and  $i\mathcal{Q}_{\tau,\kappa}(r)/r$ , respectively (here  $i$  is the imaginary unit).  $\kappa$  depends on both  $j$  and  $l$ . When  $j=l+1/2$ ,  $\kappa=l+1$  and when  $j=l-1/2$ ,  $\kappa=-l$ . The radial components of the pseudo-partial-waves can be found by applying a pseudization recipe<sup>50-52</sup> to  $\mathcal{P}_{\tau,\kappa}(r)$  and  $\mathcal{Q}_{\tau,\kappa}(r)$ . We call  $\tilde{\mathcal{P}}_{\tau,\kappa}(r)$  and  $\tilde{\mathcal{Q}}_{\tau,\kappa}(r)$

these pseudoradial components. By choosing a smooth local effective potential  $\tilde{V}_{\text{eff}}(r)$  that matches  $V_{\text{eff}}(r)$  outside the PAW spheres, the relativistic generalization of the  $\chi(r)$  functions<sup>24</sup> is obtained inverting the radial Dirac equation,

$$\chi_{\tau,\kappa}^A(r) = c \left( \frac{d}{dr} + \frac{\kappa}{r} \right) \tilde{\mathcal{Q}}_{\tau,\kappa}(r) + [\varepsilon_{\tau,\kappa} - \tilde{V}_{\text{eff}}(r)] \tilde{\mathcal{P}}_{\tau,\kappa}(r), \quad (\text{A3})$$

$$\chi_{\tau,\kappa}^B(r) = -c \left( \frac{d}{dr} - \frac{\kappa}{r} \right) \tilde{\mathcal{P}}_{\tau,\kappa}(r) + [\varepsilon_{\tau,\kappa} + 2c^2 - \tilde{V}_{\text{eff}}(r)] \tilde{\mathcal{Q}}_{\tau,\kappa}(r), \quad (\text{A4})$$

where we called  $\chi_{\tau,\kappa}^A(r)$  and  $\chi_{\tau,\kappa}^B(r)$  the radial parts of the large and small components of  $\chi_m(\mathbf{r})$ . The projectors  $\beta_{\tau,\kappa}(r)$  are calculated from  $\chi_{\tau,\kappa}(r)$  by defining the matrix  $B_{\tau,\tau'} = \langle \tilde{\mathcal{P}}_{\tau,\kappa} | \chi_{\tau',\kappa}^A \rangle + \langle \tilde{\mathcal{Q}}_{\tau,\kappa} | \chi_{\tau',\kappa}^B \rangle$  and using the relationship:  $\beta_{\tau,\kappa}(r) = \sum_{\tau'} (B^{-1})_{\tau',\tau} \chi_{\tau',\kappa}(r)$ . These projectors are orthogonal to the pseudo-wave-functions because  $\langle \beta_{\tau,\kappa} | \phi_{\tau',\kappa} \rangle$

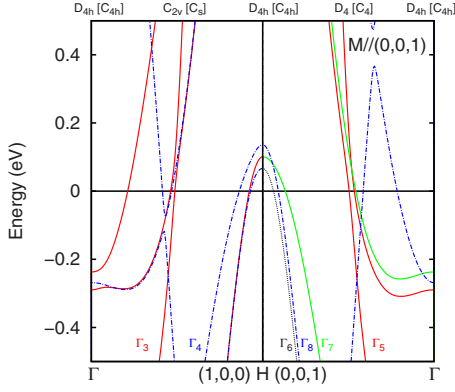


FIG. 1. (Color online) Calculated relativistic PBE-PAW band structure of ferromagnetic bcc-Fe close to the Fermi level. The bands along the  $\Gamma$ - $H$  direction are shown for both  $\mathbf{k}$  perpendicular and parallel to the magnetization direction. The zero of the energy is taken at the Fermi energy. Different colors and line types indicate bands of different symmetry with respect to the operations that do not contain time reversal (Ref. 49). The relevant group is indicated, for each line and symmetry point, in the square brackets above the figure.

$=\sum_{\tau'}(B^{-1})_{\tau',\tau}\langle\chi_{\tau',\kappa}|\phi_{\tau',\kappa}\rangle=\sum_{\tau'}(B^{-1})_{\tau',\tau}B_{\tau',\tau}=\delta_{\tau,\tau'}$ . [To simplify the notation we have indicated with  $\phi_{\tau',\kappa}(r)$  the two functions  $\tilde{\mathcal{P}}_{\tau,\kappa}(r)$  and  $\tilde{\mathcal{Q}}_{\tau,\kappa}(r)$ .

When  $\tilde{\mathcal{P}}_{\tau,\kappa}(r)$  and  $\tilde{\mathcal{Q}}_{\tau,\kappa}(r)$  are chosen independently,  $\chi_{\tau,\kappa}^B(r)$  becomes large, of order  $c$ , and the PAW data set can be used only together with the Dirac-type PAW equations. Alternatively, as proposed in Ref. 39,  $\tilde{\mathcal{P}}_{\tau,\kappa}(r)$  can be calculated by a pseudization method while  $\tilde{\mathcal{Q}}_{\tau,\kappa}(r)$  can be taken as

$$\tilde{\mathcal{Q}}_{\tau,\kappa}(r)=\frac{c}{[\varepsilon_{\tau,\kappa}+2c^2-\tilde{V}_{\text{eff}}(r)]}\left(\frac{d}{dr}-\frac{\kappa}{r}\right)\tilde{\mathcal{P}}_{\tau,\kappa}(r). \quad (\text{A5})$$

At variance with Ref. 39, we use  $\tilde{V}_{\text{eff}}(r)$  instead of the total potential of the given channel  $\kappa$ . In the PAW case there are many partial waves for each  $\kappa$  and no unique total potential. However, as long as  $\tilde{\mathcal{Q}}_{\tau,\kappa}(r)$  is continuous, the quality of the data set should be independent from how we define  $\tilde{\mathcal{Q}}_{\tau,\kappa}(r)$  so our choice should be completely equivalent to that of Ref. 39. We prefer Eq. (A5) because it has two advantages: first  $\chi_{\tau,\kappa}^B(r)$  vanishes identically together with the corresponding small component of the projector so that only the large components of the pseudo-wave-functions are necessary to evaluate the partial occupations [Eq. (33)] and second no approximation is needed for the calculation of  $\chi_{\tau,\kappa}^A(r)$ .

With this choice of the pseudo-partial-waves the projectors vanish exactly outside the PAW spheres,  $\tilde{\mathcal{Q}}_{\tau,\kappa}(r)$  is continuous and the PAW data set can be used both in the Dirac-type and in the Pauli-type formalism. The above recipe makes no approximation and therefore does not introduce additional errors, however we have not applied it because, limiting the use of the PAW data set to the Pauli-type equations, it is simpler to calculate  $\chi_{\tau,\kappa}^A(r)$  with the nonrelativistic recipe, a procedure that introduces some errors but does not

worsen the overall accuracy. If we take  $\tilde{\mathcal{Q}}_{\tau,\kappa}(r)=\frac{1}{2c}\left(\frac{d}{dr}-\frac{\kappa}{r}\right)\tilde{\mathcal{P}}_{\tau,\kappa}(r)$  we have

$$\chi_{\tau,\kappa}^A(r)=\left[\varepsilon_{\tau,\kappa}-\tilde{V}_{\text{eff}}(r)+\frac{1}{2}\frac{d^2}{dr^2}-\frac{\kappa(\kappa-1)}{2r^2}\right]\tilde{\mathcal{P}}_{\tau,\kappa}(r), \quad (\text{A6})$$

$$\chi_{\tau,\kappa}^B(r)=[\varepsilon_{\tau,\kappa}-\tilde{V}_{\text{eff}}(r)]\tilde{\mathcal{Q}}_{\tau,\kappa}(r). \quad (\text{A7})$$

Obviously, with this choice the function  $\chi_{\tau,\kappa}^A(r)$  does not vanish outside the PAW spheres and, at the border, is of order  $(v'/c)^2$ . This is because  $\tilde{\mathcal{Q}}_{\tau,\kappa}(r)$  has a jump at the border with a discontinuity of order  $(v'/c)^3$ . In the PAW Dirac-type approach these errors are unacceptable and this method has to be avoided but in the PAW Pauli-type approach they are of the same order of the errors made outside the spheres and presently still much smaller than the TEs. Using Eq. (A7), the small components  $\chi_{\tau,\kappa}^B(r)$  are quantities of order  $v_1^3/c$  and can be neglected when applied to the small components of the pseudo-wave-functions that are also of order  $v_1/c$ . The small components of the projectors  $\beta_{\tau,\kappa}^B(r)$  are of the same order of  $\chi_{\tau,\kappa}^B(r)$  because the elements of the matrix  $B_{\tau,\tau'}$  as well as of its inverse are of order one as the first term in the definition of  $B_{\tau,\tau'}$ . The second term is of order  $v_1^4/c^2$  and can be neglected. Defining the projectors  $\beta_{\tau,\kappa}^A(r)=\sum_{\tau'}(\bar{B}^{-1})_{\tau',\tau}\chi_{\tau',\kappa}^A(r)$ , where  $\bar{B}_{\tau,\tau'}$  is the matrix  $B_{\tau,\tau'}$  in which the terms of order  $v_1^4/c^2$  are neglected, we obtain projectors that are exactly orthogonal to the large component of the pseudo-wave-functions because  $\langle\beta_{\tau,\kappa}^A|\mathcal{P}_{\tau',\kappa}\rangle=\sum_{\tau'}(\bar{B}^{-1})_{\tau',\tau}\langle\chi_{\tau',\kappa}^A|\mathcal{P}_{\tau',\kappa}\rangle=\sum_{\tau'}(\bar{B}^{-1})_{\tau',\tau}\bar{B}_{\tau',\tau}=\delta_{\tau,\tau'}$ .

## APPENDIX B: SUMS OVER THE FOUR-COMPONENT SPINOR INDEXES

In this appendix, we discuss how to perform the sums over the large and small components. These sums show up both in the PAW Dirac-type equations [Eqs. (39)–(41)] as well as in the PAW Pauli-type equations [Eqs. (51)–(53)]. Sums over the  $\eta$  indexes appear in the expression of the all-electron charge and magnetization densities  $\rho^{1,l}(\mathbf{r})$ ,  $\mathbf{m}^{1,l}(\mathbf{r})$ , in the coefficients of the nonlocal PP,  $D_{l,mn}^1$  and  $\tilde{D}_{l,mn}^1$ , and in the integral of  $\tilde{V}_{\text{LOC}}^{\eta_1,\eta_2}(\mathbf{r})$  and  $\tilde{K}_{\sigma_1,\sigma_2}^{\eta_1,\eta_2}(\mathbf{r})$ . As shown below, we can replace  $Q_{mn,\eta_1,\eta_2}^l(\mathbf{r})$  with pseudized functions  $\hat{Q}_{mn,\sigma_1,\sigma_2}^l(\mathbf{r})$  that vanish everywhere except in the first upper  $2\times 2$  block. As a consequence, sums over the small components appear only for quantities calculated on the radial grids inside the spheres.

We start by considering the form of the all-electron partial waves. The partial wave  $\Phi_{m,\eta}^{l,AE}(\mathbf{r})$  can be written as

$$\Phi_{m,\eta}^{l,AE}(\mathbf{r})=\frac{1}{r}\begin{pmatrix} \mathcal{P}_{\tau,l,j}^l(r)\tilde{Y}_{l,j,m_j}^{l,\sigma}(\Omega_{\mathbf{r}}) \\ i\mathcal{Q}_{\tau,l,j}^l(r)\tilde{Y}_{2j-l,j,m_j}^{l,\sigma}(\Omega_{\mathbf{r}}) \end{pmatrix}, \quad (\text{B1})$$

where  $\tilde{Y}_{l,j,m_j}^{l,\sigma}(\Omega_{\mathbf{r}})$  are spin-angle functions whose expression is reported, for instance, in Ref. 20. The spin-angle functions

of the small and large components have different  $l$ . They are related by the relationship:  $\tilde{Y}_{2j-1,j,m_j}^l(\Omega_{\mathbf{r}}) = -\boldsymbol{\sigma} \cdot \hat{\mathbf{r}} \tilde{Y}_{l,j,m_j}^l(\Omega_{\mathbf{r}})$ , where  $\hat{\mathbf{r}} = (\mathbf{r} - \mathbf{R}_j) / |\mathbf{r} - \mathbf{R}_j|$ . This fact, together with the equation  $(\boldsymbol{\sigma} \cdot \hat{\mathbf{r}})^2 = \mathbf{1}_{2 \times 2}$ , can be used to write  $\rho^{1,l}(\mathbf{r})$  as

$$\begin{aligned} \rho^{1,l}(\mathbf{r}) &= \sum_{\tau,l,j,m_j;\tau',l',j',m'_j} \sum_{\sigma} \rho_{\tau,l,j,m_j;\tau',l',j',m'_j}^{\sigma} \frac{1}{r^2} \\ &\times [\mathcal{P}_{\tau,l,j}^l(r) \mathcal{P}_{\tau',l',j'}^l(r) \\ &+ \mathcal{Q}_{\tau,l,j}^l(r) \mathcal{Q}_{\tau',l',j'}^l(r)] \tilde{Y}_{l,j,m_j}^{*,l,\sigma}(\Omega_{\mathbf{r}}) \tilde{Y}_{l',j',m'_j}^{l,\sigma}(\Omega_{\mathbf{r}}), \end{aligned} \quad (\text{B2})$$

where we have expanded the indexes  $m$  and  $n$  introduced above with the four indexes  $\tau, l, j, m_j$  and  $\tau', l', j', m'_j$ , respectively.

For the magnetization density, we can employ the relationship  $(\boldsymbol{\sigma} \cdot \hat{\mathbf{r}}) \boldsymbol{\sigma}_i (\boldsymbol{\sigma} \cdot \hat{\mathbf{r}}) = 2\hat{\mathbf{r}}_i (\boldsymbol{\sigma} \cdot \hat{\mathbf{r}}) - \boldsymbol{\sigma}_i$  to obtain

$$\begin{aligned} \mathbf{m}_i^{1,l}(\mathbf{r}) &= \mu_B \sum_{\tau,l,j,m_j;\tau',l',j',m'_j} \sum_{\sigma_1, \sigma_2} \rho_{\tau,l,j,m_j;\tau',l',j',m'_j}^{\sigma_1, \sigma_2} \\ &\times \frac{1}{r^2} \{ [\mathcal{P}_{\tau,l,j}^l(r) \mathcal{P}_{\tau',l',j'}^l(r) \\ &+ \mathcal{Q}_{\tau,l,j}^l(r) \mathcal{Q}_{\tau',l',j'}^l(r)] \boldsymbol{\sigma}_i^{\sigma_1, \sigma_2} \\ &- \mathcal{Q}_{\tau,l,j}^l(r) \mathcal{Q}_{\tau',l',j'}^l(r) 2\hat{\mathbf{r}}_i (\boldsymbol{\sigma} \cdot \hat{\mathbf{r}})^{\sigma_1, \sigma_2} \} \\ &\times \tilde{Y}_{l,j,m_j}^{*,l,\sigma_1}(\Omega_{\mathbf{r}}) \tilde{Y}_{l',j',m'_j}^{l,\sigma_2}(\Omega_{\mathbf{r}}). \end{aligned} \quad (\text{B3})$$

For practical calculations, we apply the same approach of Ref. 27 to both the charge and the magnetization densities. Here we discuss only the latter because the charge density can be treated in a similar way. We start by recalling Eq. (6) of Ref. 27 and writing the spin-angle functions in terms of spherical harmonics. This equation is

$$\tilde{Y}_{l,j,m_j}^{l,\sigma}(\Omega_{\mathbf{r}}) = \sum_{m_l=-l}^l c_{m_j, m_l}^{\sigma, l, j} Y_{l, m_l}^{\sigma, l, j}(\Omega_{\mathbf{r}}), \quad (\text{B4})$$

where, with the notations of Ref. 27,  $c_{m_j, m_l}^{\sigma, l, j} = \alpha_{m_j}^{\sigma, l, j} U_{m_j, m_l}^{\sigma, l, j}$ ,  $\alpha_{m_j}^{\sigma, l, j}$  are the Clebsch-Gordan coefficients and  $U_{m_j, m_l}^{\sigma, l, j}$  is the unitary matrix that selects the spherical harmonics  $Y_{l, m_l}^{\sigma, l, j}$  for each  $l, j, m_j$ , and  $\sigma$ . Using this relationship, we obtain

$$\begin{aligned} \mathbf{m}_i^{1,l}(\mathbf{r}) &= \mu_B \sum_{\tau,l,j,m_j;\tau',l',j',m'_j} \sum_{\sigma_1, \sigma_2} \sum_k \sum_{m_l, m'_l} \\ &\times \boldsymbol{\sigma}_k^{\sigma_1, \sigma_2} c_{m_j, m_l}^{*, \sigma_1, l, j} c_{m'_j, m'_l}^{\sigma_2, l', j'} \rho_{\tau,l,j,m_j;\tau',l',j',m'_j}^{\sigma_1, \sigma_2} \\ &\times \frac{1}{r^2} \{ [\mathcal{P}_{\tau,l,j}^l(r) \mathcal{P}_{\tau',l',j'}^l(r) + \mathcal{Q}_{\tau,l,j}^l(r) \mathcal{Q}_{\tau',l',j'}^l(r)] \delta^{i,k} \\ &- \mathcal{Q}_{\tau,l,j}^l(r) \mathcal{Q}_{\tau',l',j'}^l(r) 2\hat{\mathbf{r}}_i \hat{\mathbf{r}}_k \} Y_{l, m_l}^{*, l, j}(\Omega_{\mathbf{r}}) Y_{l', m'_l}^{l', j'}(\Omega_{\mathbf{r}}). \end{aligned} \quad (\text{B5})$$

The partial occupations are written in terms of spin-angle functions too and can be rewritten as

$$\rho_{\tau,l,j,m_j;\tau',l',j',m'_j}^l = \sum_{\sigma_1, \sigma_2} \sum_{m_l, m'_l} c_{m_j, m_l}^{\sigma_1, l, j} c_{m'_j, m'_l}^{*, \sigma_2, l', j'} \rho_{\tau,l,j,m_l;\tau',l',j',m'_l}^{l, \sigma_1, \sigma_2}, \quad (\text{B6})$$

where  $\tilde{\rho}_{\tau,l,j,m_l;\tau',l',j',m'_l}^{l, \sigma_1, \sigma_2}$  are partial occupations calculated as in the SR case, with projectors defined by spherical harmonics<sup>27</sup>

$$\tilde{\rho}_{\tau,l,j,m_l;\tau',l',j',m'_l}^{l, \sigma_1, \sigma_2} = \sum_i \langle \tilde{\Psi}_{i, \sigma_1}^A | \beta_{\tau, l, j}^{l, A} Y_{l, m_l}^{\sigma_1, l, j} \rangle \langle \beta_{\tau', l', j'}^{l', A} Y_{l', m'_l}^{\sigma_2, l', j'} | \tilde{\Psi}_{i, \sigma_2}^A \rangle. \quad (\text{B7})$$

We assumed that the small components of the projectors are negligible (Pauli-type case) or vanish (Dirac-type case). When this does not happen, Eqs. (B6) and (B7) are more complicated but we do not need them. Following now Ref. 27 and introducing the functions  $f_{l,j,m_l;l,j,m_l}^{\sigma_1, \sigma_2} = \sum_{m_j} c_{m_j, m_l}^{\sigma_1, l, j} c_{m_j, m_l}^{*, \sigma_2, l, j}$  and the partial occupations,

$$\begin{aligned} \rho_{\tau,l,j,m_l;\tau',l',j',m'_l}^{l, \sigma_1, \sigma_2} &= \sum_{\sigma_3, \sigma_4} \sum_{m_l, m'_l} f_{l,j,m_l;l,j,m_l}^{\sigma_3, \sigma_1} \\ &\times f_{l',j',m'_l;l',j',m'_l}^{\sigma_2, \sigma_4} \tilde{\rho}_{\tau,l,j,m_l;\tau',l',j',m'_l}^{l, \sigma_3, \sigma_4}, \end{aligned} \quad (\text{B8})$$

we can calculate the magnetization density making sums over the  $m_l$  and  $m'_l$  ( $-l \leq m_l \leq l$  and  $-l' \leq m'_l \leq l'$ ) instead of  $m_j$  and  $m'_j$  ( $-j \leq m_j \leq j$  and  $-j' \leq m'_j \leq j'$ ). We have

$$\begin{aligned} \mathbf{m}_i^{1,l}(\mathbf{r}) &= \mu_B \sum_{\tau,l,j,m_l;\tau',l',j',m'_l} \sum_k \sum_{\sigma_1, \sigma_2} \boldsymbol{\sigma}_k^{\sigma_1, \sigma_2} \rho_{\tau,l,j,m_l;\tau',l',j',m'_l}^{l, \sigma_1, \sigma_2} \\ &\times \frac{1}{r^2} \{ [\mathcal{P}_{\tau,l,j}^l(r) \mathcal{P}_{\tau',l',j'}^l(r) + \mathcal{Q}_{\tau,l,j}^l(r) \mathcal{Q}_{\tau',l',j'}^l(r)] \delta^{i,k} \\ &- \mathcal{Q}_{\tau,l,j}^l(r) \mathcal{Q}_{\tau',l',j'}^l(r) 2\hat{\mathbf{r}}_i \hat{\mathbf{r}}_k \} Y_{l, m_l}^{*, l, j}(\Omega_{\mathbf{r}}) Y_{l', m'_l}^{l', j'}(\Omega_{\mathbf{r}}). \end{aligned} \quad (\text{B9})$$

This expression and the equivalent expression for  $\tilde{\mathbf{m}}_i^{1,l}(\mathbf{r}) + \hat{\mathbf{m}}_i^{1,l}(\mathbf{r})$  have been implemented in QE.<sup>41</sup>

Let us now discuss how to define the augmentation functions. These functions have to satisfy two constraints. On one hand, they have to be as smooth as possible to be described in the real-space mesh and on the other hand they have to give compensation charges with the same multipole moments as  $\rho^{1,l}(\mathbf{r}) - \tilde{\rho}^{1,l}(\mathbf{r})$ . These charge-density differences are equal to

$$\begin{aligned} \rho^{1,l}(\mathbf{r}) - \tilde{\rho}^{1,l}(\mathbf{r}) &= \sum_{\tau,l,j,m_j;\tau',l',j',m'_j} \sum_{\sigma} \rho_{\tau,l,j,m_j;\tau',l',j',m'_j}^{\sigma} \\ &\times A_{\tau,l,j;\tau',l',j'}^l(\mathbf{r}) \tilde{Y}_{l,j,m_j}^{*, l, \sigma}(\Omega_{\mathbf{r}}) \tilde{Y}_{l',j',m'_j}^{l, \sigma}(\Omega_{\mathbf{r}}), \end{aligned} \quad (\text{B10})$$

where we used the notation  $A_{\tau,l,j;\tau',l',j'}^l(\mathbf{r}) = \frac{1}{r^2} [\mathcal{P}_{\tau,l,j}^l(r) \mathcal{P}_{\tau',l',j'}^l(r) + \mathcal{Q}_{\tau,l,j}^l(r) \mathcal{Q}_{\tau',l',j'}^l(r) - \tilde{\mathcal{P}}_{\tau,l,j}^l(r) \tilde{\mathcal{P}}_{\tau',l',j'}^l(r) - \tilde{\mathcal{Q}}_{\tau,l,j}^l(r) \tilde{\mathcal{Q}}_{\tau',l',j'}^l(r)]$  that is suitable to the PAW Dirac-type case. As suggested by Eq. (46), in the PAW Pauli-type case

the term  $\tilde{Q}_{\tau,l,j}^I(r)\tilde{Q}_{\tau',l',j'}^I(r)$  is omitted whereas the small components of the all-electron partial waves are included only inside the PAW spheres.

Equation (B10) can be rewritten introducing the spherical harmonics. Following stepwise the derivation of Eq. (B9), we have

$$\begin{aligned} \rho^{1,l}(\mathbf{r}) - \tilde{\rho}^{1,l}(\mathbf{r}) &= \sum_{\tau,l,j,m_j;\tau',l',j',m'_j} \sum_{\sigma} \rho_{\tau,l,j,m_j;\tau',l',j',m'_j}^{l,\sigma,\sigma} \\ &\times A_{\tau,l,j;\tau',l',j'}^I(r) Y_{l,m_j}^{l*}(\Omega_{\mathbf{r}}) Y_{l',m'_j}^{l'}(\Omega_{\mathbf{r}}). \end{aligned} \quad (\text{B11})$$

Expanding the product of two spherical harmonics into spherical harmonics,

$$\begin{aligned} Y_{l,m_j}^{l*}(\Omega_{\mathbf{r}}) Y_{l',m'_j}^{l'}(\Omega_{\mathbf{r}}) \\ = \sum_{L=|l-l'|}^{l+l'} \sum_{M=-L}^L a(l,m_j;l',m'_j;L,M) Y_{L,M}^{l+l'}(\Omega_{\mathbf{r}}), \end{aligned} \quad (\text{B12})$$

we can proceed as in the SR case,<sup>40</sup> replacing each function  $A_{\tau,l,j;\tau',l',j'}^I(r)$  with many functions, one for each  $L$  so as to conserve the  $L$  multipole moment. We call  $\tilde{A}_{\tau,l,j;\tau',l',j'}^{l,L}(r)$  these functions that can be constructed as described in Ref. 15 or with any equivalent method. The final expression of the compensation charge is

$$\hat{\rho}^l(\mathbf{r}) = \sum_{\tau,l,j,m_j;\tau',l',j',m'_j} \sum_{\sigma} \rho_{\tau,l,j,m_j;\tau',l',j',m'_j}^{l,\sigma,\sigma} \hat{Q}_{\tau,l,j,m_j;\tau',l',j',m'_j}^l(\mathbf{r}), \quad (\text{B13})$$

where the augmentation functions are

$$\begin{aligned} \hat{Q}_{\tau,l,j,m_j;\tau',l',j',m'_j}^l(\mathbf{r}) \\ = \sum_{L,M} \tilde{A}_{\tau,l,j;\tau',l',j'}^{l,L}(r) a(l,m_j;l',m'_j;L,M) Y_{L,M}^{l+l'}(\Omega_{\mathbf{r}}) \end{aligned} \quad (\text{B14})$$

in close analogy with the SR case. The augmentation functions  $\hat{Q}_{mn,\eta_1,\eta_2}^l(\mathbf{r})$  used in Eqs. (41) and (51) and in the definition of  $\tilde{K}_{\eta_3,\eta_4}^{\eta_1,\eta_2}(\mathbf{r})$  can be constructed starting from  $\hat{Q}_{\tau,l,j,m_j;\tau',l',j',m'_j}^l(\mathbf{r})$ . The way in which we separate the angular and spin components of  $\hat{Q}_{mn,\eta_1,\eta_2}^l(\mathbf{r})$  is to a certain extent arbitrary, provided that the compensation charges  $\hat{\rho}^l(\mathbf{r})$  have the same multipole moments as  $\rho^{1,l}(\mathbf{r}) - \tilde{\rho}^{1,l}(\mathbf{r})$ . For computational convenience, we defined augmentation functions that vanish everywhere except in the first upper  $2 \times 2$  block. We take

$$\begin{aligned} \hat{Q}_{\tau,l,j,m_j;\tau',l',j',m'_j;\sigma_1,\sigma_2}^l(\mathbf{r}) \\ = \sum_{m_j,m'_j} c_{m_j,m'_j}^{*,\sigma_1,l,j} c_{m'_j,m_j}^{\sigma_2,l',j'} \hat{Q}_{\tau,l,j,m_j;\tau',l',j',m'_j}^l(\mathbf{r}) \end{aligned} \quad (\text{B15})$$

and zero elsewhere. With this definition,  $\hat{\rho}_{\eta_1,\eta_2}^l(\mathbf{r})$  becomes

$$\hat{\rho}_{\eta_1,\eta_2}^l(\mathbf{r}) = \begin{pmatrix} \sum_{\tau,l,j,m_j;\tau',l',j',m'_j} \rho_{\tau,l,j,m_j;\tau',l',j',m'_j}^l \hat{Q}_{\tau,l,j,m_j;\tau',l',j',m'_j;\sigma_1,\sigma_2}^l(\mathbf{r}) & 0 \\ 0 & 0 \end{pmatrix} \quad (\text{B16})$$

inside the spheres, and  $\hat{\rho}_{\eta_1,\eta_2}^l(\mathbf{r}) = \sum_l \hat{\rho}_{\eta_1,\eta_2}^l(\mathbf{r} - \mathbf{R}_l)$  in the real-space mesh. Although the lower and the off-diagonal  $2 \times 2$  blocks of the compensation density matrices are forced to vanish, the compensation charges have the correct multipole moments and this is a sufficient condition to have the correct electrostatics so with this choice we are not introducing any additional error.

Finally, we discuss how to calculate  $D_{l,mn}^1$  and the nonlocal PP terms  $\sum_{l,mn} D_{l,mn}^1 |\beta_{m,\sigma_1}^{l,A}\rangle \langle \beta_{n,\sigma_2}^{l,A}|$ .  $D_{l,mn}^1$  has two parts, one due to the kinetic-energy operator and one due to the term  $V_{\text{LOC}}^{l,\eta_1,\eta_2}$ . They are quite different and are dealt with separately. The kinetic-energy part presents no difficulty because the spherically symmetric Dirac operator can be calculated in the isolated atom. The all-electron partial waves solve the atomic Dirac-type equations so the sum over the spin components and the angular integral can be carried out analytically. We

have  $\sum_{\eta_1,\eta_2} \langle \Phi_{m,\eta_1}^{l,AE} | T_D^{\eta_1,\eta_2} | \Phi_{n,\eta_2}^{l,AE} \rangle_{\Omega} = \delta_{l,l'} \delta_{j,j'} \delta_{m_j,m'_j} T_{D,\tau,\tau'}^{l,l,j}$  where

$$\begin{aligned} T_{D,\tau,\tau'}^{l,l,j} &= \int_0^{r_s} dr [\mathcal{P}_{\tau,l,j}^l(r) \mathcal{P}_{\tau',l,j}^l(r) + \mathcal{Q}_{\tau,l,j}^l(r) \mathcal{Q}_{\tau',l,j}^l(r)] \\ &\times [\varepsilon_{\tau',l,j} - V_{\text{eff,at}}^l(r)]. \end{aligned} \quad (\text{B17})$$

$r_s$  is the radius of the PAW sphere,  $\varepsilon_{\tau',l,j}$  is the energy at which the partial waves and projectors have been constructed, and  $V_{\text{eff,at}}^l(r)$  is the atomic effective all-electron potential.  $T_{D,\tau,\tau'}^{l,l,j}$  are calculated together with the partial waves and projectors during the PAW data set generation. They

have the same structure of the unscreened coefficients of the nonlocal FR US-PPs. Following Ref. 27, we can write

$$\begin{aligned} & \sum_{l,mn} \sum_{\eta_1, \eta_2} \langle \Phi_{m, \eta_1}^{I,AE} | T_D^{\eta_1, \eta_2} | \Phi_{n, \eta_2}^{I,AE} \rangle_{\Omega} | \beta_{m, \sigma_1}^{I,A} \rangle \langle \beta_{n, \sigma_2}^{I,A} | \\ &= \sum_I \sum_{\tau, l, j, m_l} \sum_{\tau', l', j', m'_l} T_{D, \tau, l, j, m_l; \tau', l', j', m'_l}^{I, \sigma_1, \sigma_2} | \beta_{\tau, l, j}^{I,A} Y_{l, m_l}^{I'} \rangle \\ & \quad \times \langle \beta_{\tau', l', j'}^{I,A} Y_{l', m'_l}^{I'} |, \end{aligned} \quad (\text{B18})$$

where

$$T_{D, \tau, l, j, m_l; \tau', l', j', m'_l}^{I, \sigma_1, \sigma_2} = T_{D, \tau, \tau'}^{I, l, j} f_{l, j, m_l; l', j', m'_l}^{\sigma_1, \sigma_2} \delta_{l, l'} \delta_{j, j'}, \quad (\text{B19})$$

so this term has the same expression as the nonlocal part of a SR US-PP but with spin-dependent nonlocal PP coefficients.

In general  $V_{\text{LOC}}^{I, \eta_1, \eta_2}(\mathbf{r})$  is not spherically symmetric but it is block diagonal and does not couple the large and small components of the partial waves. With the same techniques introduced in this appendix, we can write

$$\begin{aligned} & \sum_{\eta_1, \eta_2} \langle \Phi_{m, \eta_1}^{I,AE} | V_{\text{LOC}}^{I, \eta_1, \eta_2} | \Phi_{n, \eta_2}^{I,AE} \rangle_{\Omega} \\ &= \sum_{\sigma_1, \sigma_2} \langle \mathcal{P}_{\tau, l, j}^I \tilde{Y}_{l, j, m_j}^{I, \sigma_1} | V_{\text{LOC}}^{I, \sigma_1, \sigma_2} | \mathcal{P}_{\tau', l', j'}^I \tilde{Y}_{l', j', m'_j}^{I, \sigma_2} \rangle_{\Omega} \\ &+ \sum_{\sigma_1, \sigma_2} \langle \mathcal{Q}_{\tau, l, j}^I \tilde{Y}_{l, j, m_j}^{I, \sigma_1} | V_{\text{LOC}}^{I, \sigma_1, \sigma_2} | \mathcal{Q}_{\tau', l', j'}^I \tilde{Y}_{l', j', m'_j}^{I, \sigma_2} \rangle_{\Omega} \\ &+ \sum_{\sigma_1, \sigma_2} \langle \mathcal{Q}_{\tau, l, j}^I \tilde{Y}_{l, j, m_j}^{I, \sigma_1} | 2\mu_B \mathbf{B}_{\text{xc}}^I \cdot \hat{\mathbf{r}}(\boldsymbol{\sigma} \cdot \hat{\mathbf{r}})^{\sigma_1, \sigma_2} | \mathcal{Q}_{\tau', l', j'}^I \tilde{Y}_{l', j', m'_j}^{I, \sigma_2} \rangle_{\Omega}. \end{aligned} \quad (\text{B20})$$

This complete expression, which is needed in a magnetic solid, can be simplified by carrying out the angular integrals analytically. We first write the angular dependence of the integrand function by introducing the spherical harmonics,

$$\begin{aligned} & \sum_{\eta_1, \eta_2} \langle \Phi_{m, \eta_1}^{I,AE} | V_{\text{LOC}}^{I, \eta_1, \eta_2} | \Phi_{n, \eta_2}^{I,AE} \rangle_{\Omega} \\ &= \sum_{\sigma_1, \sigma_2} \sum_{m_l, m'_l} c_{m_j, m_l}^{*, \sigma_1, l, j} c_{m'_j, m'_l}^{\sigma_2, l', j'} \int_{\Omega_I} \frac{d^3 r}{r^2} \{ [\mathcal{P}_{\tau, l, j}^I(r) \mathcal{P}_{\tau', l', j'}^I(r) \\ &+ \mathcal{Q}_{\tau, l, j}^I(r) \mathcal{Q}_{\tau', l', j'}^I(r)] V_{\text{LOC}}^{I, \sigma_1, \sigma_2}(\mathbf{r}) \\ &+ \mathcal{Q}_{\tau, l, j}^I(r) \mathcal{Q}_{\tau', l', j'}^I(r) 2\mu_B \mathbf{B}_{\text{xc}}^I \cdot \hat{\mathbf{r}}(\boldsymbol{\sigma} \cdot \hat{\mathbf{r}})^{\sigma_1, \sigma_2} \} \\ & \quad \times Y_{l, m_l}^{I*}(\Omega_{\mathbf{r}}) Y_{l', m'_l}^{I'}(\Omega_{\mathbf{r}}), \end{aligned} \quad (\text{B21})$$

then we expand  $V_{\text{LOC}}^{I, \sigma_1, \sigma_2}(\mathbf{r})$  and  $G(\mathbf{r})^{I, \sigma_1, \sigma_2} = 2\mu_B \mathbf{B}_{\text{xc}}^I \cdot \hat{\mathbf{r}}(\boldsymbol{\sigma} \cdot \hat{\mathbf{r}})^{\sigma_1, \sigma_2}$  in spherical harmonics,

$$V_{\text{LOC}}^{I, \sigma_1, \sigma_2}(\mathbf{r}) = \sum_{L, M} V_{\text{LOC}, L, M}^{I, \sigma_1, \sigma_2}(r) Y_{L, M}^{I'}(\Omega_{\mathbf{r}}), \quad (\text{B22})$$

$$G^{I, \sigma_1, \sigma_2}(\mathbf{r}) = \sum_{L, M} G_{L, M}^{I, \sigma_1, \sigma_2}(r) Y_{L, M}^{I'}(\Omega_{\mathbf{r}}). \quad (\text{B23})$$

Using the expansion [Eq. (B12)], we obtain

$$\begin{aligned} & \sum_{\eta_1, \eta_2} \langle \Phi_{m, \eta_1}^{I,AE} | V_{\text{LOC}}^{I, \eta_1, \eta_2} | \Phi_{n, \eta_2}^{I,AE} \rangle_{\Omega} \\ &= \sum_{\sigma_3, \sigma_4} \sum_{m_l, m'_l} c_{m_j, m_l}^{*, \sigma_3, l, j} c_{m'_j, m'_l}^{\sigma_4, l', j'} \bar{D}_{\text{LOC}, \tau, l, j, m_l; \tau', l', j', m'_l}^{I, \sigma_3, \sigma_4}, \end{aligned} \quad (\text{B24})$$

where

$$\begin{aligned} \bar{D}_{\text{LOC}, \tau, l, j, m_l; \tau', l', j', m'_l}^{I, \sigma_3, \sigma_4} &= \sum_{L, M} \int_0^{r_s} dr \{ [\mathcal{P}_{\tau, l, j}^I(r) \mathcal{P}_{\tau', l', j'}^I(r) \\ &+ \mathcal{Q}_{\tau, l, j}^I(r) \mathcal{Q}_{\tau', l', j'}^I(r)] V_{\text{LOC}, L, M}^{I, \sigma_3, \sigma_4}(r) \\ &+ \mathcal{Q}_{\tau, l, j}^I(r) \mathcal{Q}_{\tau', l', j'}^I(r) \\ & \quad \times G_{L, M}^{I, \sigma_3, \sigma_4}(r) \} a(l, m_l; l', m'_l; L, M). \end{aligned} \quad (\text{B25})$$

In these expressions, for simplicity, we used real spherical harmonics but a straightforward generalization would allow the use of complex spherical harmonics. We can now write the contribution of this term to the nonlocal PP. We have

$$\begin{aligned} & \sum_{l, mn} \sum_{\eta_1, \eta_2} \langle \Phi_{m, \eta_1}^{I,AE} | V_{\text{LOC}}^{I, \eta_1, \eta_2} | \Phi_{n, \eta_2}^{I,AE} \rangle_{\Omega} | \beta_{m, \sigma_1}^{I,A} \rangle \langle \beta_{n, \sigma_2}^{I,A} | \\ &= \sum_I \sum_{\tau, l, j, m_l} \sum_{\tau', l', j', m'_l} D_{\text{LOC}, \tau, l, j, m_l; \tau', l', j', m'_l}^{I, \sigma_1, \sigma_2} | \beta_{\tau, l, j}^{I,A} Y_{l, m_l}^{I'} \rangle \\ & \quad \times \langle \beta_{\tau', l', j'}^{I,A} Y_{l', m'_l}^{I'} |, \end{aligned} \quad (\text{B26})$$

where

$$\begin{aligned} D_{\text{LOC}, \tau, l, j, m_l; \tau', l', j', m'_l}^{I, \sigma_1, \sigma_2} &= \sum_{\sigma_3, \sigma_4} \sum_{m_l, m'_l} f_{l, j, m_l; l', j', m'_l}^{\sigma_3, \sigma_4} f_{l', j', m'_l; l', j', m'_l}^{\sigma_4, \sigma_2} \\ & \quad \times \bar{D}_{\text{LOC}, \tau, l, j, m_l; \tau', l', j', m'_l}^{I, \sigma_3, \sigma_4}, \end{aligned} \quad (\text{B27})$$

so also the term due to  $V_{\text{LOC}}^{\eta_1, \eta_2}$  has the same form of a nonlocal SR US-PP with spin-dependent coefficients and do not introduce any complication into existing electronic structure codes.

In nonmagnetic solids several simplifications occur. The last term in the square bracket of Eq. (B25) vanishes and  $V_{\text{LOC}}^{\sigma_1, \sigma_2}(\mathbf{r})$  is diagonal in the spin indexes, so we obtain

$$\begin{aligned} \bar{D}_{\text{LOC}, \tau, l, j, m_l; \tau', l', j', m'_l}^{I, \sigma_3, \sigma_4} &= \delta^{\sigma_3, \sigma_4} \sum_{L, M} \int_0^{r_s} dr \{ [\mathcal{P}_{\tau, l, j}^I(r) \mathcal{P}_{\tau', l', j'}^I(r) \\ &+ \mathcal{Q}_{\tau, l, j}^I(r) \mathcal{Q}_{\tau', l', j'}^I(r)] V_{\text{eff}, L, M}^I(r) \} \\ & \quad \times a(l, m_l; l', m'_l; L, M). \end{aligned} \quad (\text{B28})$$

In the US-PPs case this term is calculated in the nonmagnetic isolated atom, so  $V_{\text{eff}}^I(\mathbf{r})$  is spherically symmetric. In

Eq. (B20) the expectation values between spin-angle functions are nonzero only when  $l=l'$ ,  $j=j'$ , and  $m_j=m'_j$  and we have

$$\begin{aligned} & \sum_{\eta_1, \eta_2} \langle \Phi_{m, \eta_1}^{I, AE} | V_{\text{LOC}}^{I, \eta_1, \eta_2} | \Phi_{n, \eta_2}^{I, AE} \rangle \\ &= \delta_{l, l'} \delta_{j, j'} \delta_{m_j, m'_j} \int_0^{r_s} dr [\mathcal{P}_{\tau, l, j}^I(r) \mathcal{P}_{\tau', l', j'}^I(r) \\ &+ \mathcal{Q}_{\tau, l, j}^I(r) \mathcal{Q}_{\tau', l', j'}^I(r)] V_{\text{eff,at}}^I(r). \end{aligned} \quad (\text{B29})$$

This term can be combined with the kinetic-energy term to give the US expression of  $D_{l, mn}^I$ ,

$$\begin{aligned} D_{l, \tau, l, j, m_j; \tau', l', j', m'_j}^I &= \delta_{l, l'} \delta_{j, j'} \delta_{m_j, m'_j} \varepsilon_{\tau', l, j} \int_0^{r_s} dr [\mathcal{P}_{\tau, l, j}^I(r) \mathcal{P}_{\tau', l', j'}^I(r) \\ &+ \mathcal{Q}_{\tau, l, j}^I(r) \mathcal{Q}_{\tau', l', j'}^I(r)]. \end{aligned} \quad (\text{B30})$$

Similar considerations as the ones reported for  $D_{l, mn}^I$  apply also to  $\tilde{D}_{l, mn}^I$  that, having no sum over the four components indexes, is simpler to deal with.

- <sup>1</sup>P. Hohenberg and W. Kohn, *Phys. Rev.* **136**, B864 (1964); W. Kohn and L. J. Sham, *ibid.* **140**, A1133 (1965).
- <sup>2</sup>A. H. MacDonald and S. H. Vosko, *J. Phys. C* **12**, 2977 (1979); A. K. Rajagopal and J. Callaway, *Phys. Rev. B* **7**, 1912 (1973).
- <sup>3</sup>D. D. Koelling and B. N. Harmon, *J. Phys. C* **10**, 3107 (1977).
- <sup>4</sup>C. Li, A. J. Freeman, H. J. F. Jansen, and C. L. Fu, *Phys. Rev. B* **42**, 5433 (1990).
- <sup>5</sup>Ph. Kurz, F. Förster, L. Nordström, G. Bihlmayer, and S. Blügel, *Phys. Rev. B* **69**, 024415 (2004).
- <sup>6</sup>J. Anton, B. Fricke, and E. Engel, *Phys. Rev. A* **69**, 012505 (2004).
- <sup>7</sup>P. Pyykkö, *Chem. Rev.* **88**, 563 (1988).
- <sup>8</sup>P. Cortona, S. Doniach, and C. Sommers, *Phys. Rev. A* **31**, 2842 (1985).
- <sup>9</sup>E. Engel, T. Auth, and R. M. Dreizler, *Phys. Rev. B* **64**, 235126 (2001).
- <sup>10</sup>J. Anton, T. Jacob, B. Fricke, and E. Engel, *Phys. Rev. Lett.* **89**, 213001 (2002).
- <sup>11</sup>S. Bei der Kellen and A. J. Freeman, *Phys. Rev. B* **54**, 11187 (1996).
- <sup>12</sup>V. Theileis and H. Bross, *Phys. Rev. B* **62**, 13338 (2000).
- <sup>13</sup>P. Strange, H. Ebert, J. B. Staunton, and B. L. Gyorffy, *J. Phys.: Condens. Matter* **1**, 2959 (1989).
- <sup>14</sup>P. E. Blöchl, *Phys. Rev. B* **50**, 17953 (1994).
- <sup>15</sup>G. Kresse and D. Joubert, *Phys. Rev. B* **59**, 1758 (1999).
- <sup>16</sup>D. Hobbs, G. Kresse, and J. Hafner, *Phys. Rev. B* **62**, 11556 (2000).
- <sup>17</sup>A. Dal Corso, *Phys. Rev. B* **81**, 075123 (2010).
- <sup>18</sup>P. Carrier and S.-H. Wei, *Phys. Rev. B* **70**, 035212 (2004).
- <sup>19</sup>L. L. Foldy and S. A. Wouthuysen, *Phys. Rev. B* **78**, 29 (1950).
- <sup>20</sup>B. H. Bransden and C. J. Joachain, *Quantum Mechanics*, 2nd ed. (Prentice-Hall, Englewood Cliffs, NJ, 2000).
- <sup>21</sup>E. van Lenthe, E. J. Baerends, and J. G. Snijders, *J. Chem. Phys.* **99**, 4597 (1993).
- <sup>22</sup>E. van Lenthe, E. J. Baerends, and J. G. Snijders, *J. Chem. Phys.* **101**, 9783 (1994).
- <sup>23</sup>P. Romaniello and P. L. de Boeij, *J. Chem. Phys.* **127**, 174111 (2007).
- <sup>24</sup>D. Vanderbilt, *Phys. Rev. B* **41**, 7892 (1990).
- <sup>25</sup>L. Kleinman, *Phys. Rev. B* **21**, 2630 (1980).
- <sup>26</sup>G. B. Bachelet and M. Schlüter, *Phys. Rev. B* **25**, 2103 (1982).
- <sup>27</sup>A. Dal Corso and A. Mosca Conte, *Phys. Rev. B* **71**, 115106 (2005).
- <sup>28</sup>A. Dal Corso, *Phys. Rev. B* **76**, 054308 (2007).
- <sup>29</sup>A. Dal Corso, *J. Phys.: Condens. Matter* **20**, 445202 (2008).
- <sup>30</sup>R. Mazzarello, A. Dal Corso, and E. Tosatti, *Surf. Sci.* **602**, 893 (2008).
- <sup>31</sup>G. Sclauzero, A. Dal Corso, A. Smogunov, and E. Tosatti, *Phys. Rev. B* **78**, 085421 (2008).
- <sup>32</sup>A. Dal Corso, A. Smogunov, and E. Tosatti, *Phys. Rev. B* **74**, 045429 (2006).
- <sup>33</sup>X. Wang, J. R. Yates, I. Souza, and D. Vanderbilt, *Phys. Rev. B* **74**, 195118 (2006).
- <sup>34</sup>Y. Yao, L. Kleinman, A. H. MacDonald, J. Sinova, T. Jungwirth, D.-s. Wang, E. Wang, and Q. Niu, *Phys. Rev. Lett.* **92**, 037204 (2004).
- <sup>35</sup>All numerical results reported in this paper have been obtained with  $c=137.03599966$  a.u.
- <sup>36</sup>U. von Barth and L. Hedin, *J. Phys. C* **5**, 1629 (1972).
- <sup>37</sup>T. Oda, A. Pasquarello, and R. Car, *Phys. Rev. Lett.* **80**, 3622 (1998).
- <sup>38</sup>R. Gebauer and S. Baroni, *Phys. Rev. B* **61**, R6459 (2000).
- <sup>39</sup>E. Engel, A. Höck, and S. Varga, *Phys. Rev. B* **63**, 125121 (2001).
- <sup>40</sup>K. Laasonen, A. Pasquarello, R. Car, C. Lee, and D. Vanderbilt, *Phys. Rev. B* **47**, 10142 (1993).
- <sup>41</sup>P. Giannozzi, S. Baroni, N. Bonini, M. Calandra, R. Car, C. Cavazzoni, D. Ceresoli, G. L. Chiarotti, M. Cococcioni, I. Dabo, A. Dal Corso, S. de Gironcoli, S. Fabris, G. Fratesi, R. Gebauer, U. Gerstmann, C. Gougoussis, A. Kokalj, M. Lazzeri, L. Martin-Samos, N. Marzari, F. Mauri, R. Mazzarello, S. Paolini, A. Pasquarello, L. Paulatto, C. Sbraccia, S. Scandolo, G. Sclauzero, A. P. Seitsonen, A. Smogunov, P. Umari, and R. M. Wentzcovitch, *J. Phys.: Condens. Matter* **21**, 395502 (2009). See <http://www.quantum-espresso.org>. The formulas described in the paper have been implemented starting from QE-4.2 where the collinear nonrelativistic PAW method was already implemented, L. Paulatto, S. de Gironcoli, G. Fratesi, and R. Mazzarello (unpublished).
- <sup>42</sup>J. P. Perdew and A. Zunger, *Phys. Rev. B* **23**, 5048 (1981).
- <sup>43</sup>J. P. Perdew, K. Burke, and M. Ernzerhof, *Phys. Rev. Lett.* **77**, 3865 (1996).
- <sup>44</sup>PAW data sets without semicore states have been generated with the valence electronic configurations:  $4s_{1/2}^{1.7}4p_{1/2}^04p_{3/2}^03d_{3/2}^43d_{5/2}^{2.3}$  (Fe),  $6s_{1/2}^16p_{1/2}^06p_{3/2}^05d_{3/2}^45d_{5/2}^5$  (Pt), and  $6s_{1/2}^16p_{1/2}^06p_{3/2}^05d_{3/2}^45d_{5/2}^6$  (Au). The core radii (in bohr atomic unit) are Fe  $r_s=2.2$ ,  $r_p=2.2$ ,  $r_d=1.8$ , Pt  $r_s=2.4$ ,  $r_p=2.5$ ,  $r_d=2.2$ , and Au  $r_s=2.3$ ,  $r_p=2.4$ ,  $r_d=2.2$ . The nonlocal channels are fitted

at the eigenvalue and at  $\epsilon_s=2.3$  Ry,  $\epsilon_p=2.5$  Ry,  $\epsilon_d=-0.3$  Ry in Fe, at  $\epsilon_s=2.5$  Ry,  $\epsilon_p=3.5$  Ry,  $\epsilon_d=0.8$  Ry in Pt, and at  $\epsilon_s=2.3$  Ry,  $\epsilon_p=3.6$  Ry,  $\epsilon_d=-0.3$  Ry in Au. NLCC is used in Fe, Pt, and Au ( $r_c=1.2, 1.6, 1.6$ ). The local potential is the all-electron potential smoothed before  $r_{loc}=2.1, 2.4, 2.4$  in Fe, Au, and Pt, respectively. PAW data sets with semicore states have been generated with the valence electronic configurations:  $3s_{1/2}^2 3p_{1/2}^2 3p_{3/2}^4 4s_{1/2}^2 4p_{1/2}^0 4p_{3/2}^0 3d_{3/2}^4 3d_{5/2}^2$  (Fe),  $5s_{1/2}^2 5p_{1/2}^2 5p_{3/2}^4 6s_{1/2}^0 6p_{1/2}^0 6p_{3/2}^0 5d_{3/2}^4 5d_{5/2}^2$  (Pt), and  $5s_{1/2}^2 5p_{1/2}^2 5p_{3/2}^4 6s_{1/2}^0 6p_{1/2}^0 6p_{3/2}^0 5d_{3/2}^4 5d_{5/2}^2$  (Au). The core radii are Fe  $r_{3s}=1.3$ ,  $r_{4s}=1.4$ ,  $r_{3p}=1.3$ ,  $r_{4p}=1.6$ ,  $r_d=2.0$ , Pt  $r_s=1.6$ ,  $r_{5p}=1.6$ ,  $r_{6p}=1.8$ ,  $r_d=2.3$ , and Au  $r_{5s}=1.5$ ,  $r_{6s}=1.6$ ,  $r_{5p}=1.4$ ,  $r_{5p}=1.9$ ,  $r_d=2.3$ . The nonlocal channels are fitted at the eigenvalues and at  $\epsilon_d=-0.4$  Ry in Fe, at  $\epsilon_d=-0.3$  Ry in Pt, and at  $\epsilon_d=-0.3$  Ry in Au. NLCC is used in Fe, Pt, and Au ( $r_c=0.6, 1.0, 1.0$ ). The local potential is the all-electron potential

smoothed before  $r_{loc}=1.8, 1.8, 1.6$  in Fe, Au, and Pt, respectively. PAW data sets are generated by the *ld1* atomic code generalized to relativistic PAW as explained in Appendix A.

- <sup>45</sup>P. Haas, F. Tran, and P. Blaha, *Phys. Rev. B* **79**, 085104 (2009).  
<sup>46</sup>E. G. Moroni, G. Kresse, J. Hafner, and J. Furthmüller, *Phys. Rev. B* **56**, 15629 (1997).  
<sup>47</sup>A. Khein, D. J. Singh, and C. J. Umrigar, *Phys. Rev. B* **51**, 4105 (1995).  
<sup>48</sup>At the experimental lattice constant the magnetic moment is  $\mu=2.22 \mu_B$ .  
<sup>49</sup>L. D. Landau and E. M. Lifshitz, *Electrodynamics of continuous Media* (Pergamon Press, Oxford, 1960).  
<sup>50</sup>N. Troullier and J. L. Martins, *Phys. Rev. B* **43**, 1993 (1991).  
<sup>51</sup>A. M. Rappe, K. M. Rabe, E. Kaxiras, and J. D. Joannopoulos, *Phys. Rev. B* **41**, 1227 (1990).  
<sup>52</sup>D. Vanderbilt, *Phys. Rev. B* **32**, 8412 (1985).